SAFETY AND STABILITY
IN
CONCRETE BARREL SHELL
ROOF STRUCTURES

David Frederick Kelley

A Thesis
Presented to the Faculty of Princeton University
in Candidacy for the Degree
Master of Science in Engineering

Recommended for Acceptance by the
Department of Civil Engineering and Operations Research

October 1991

I hereby declare that I am the sole author of this thesis.

I authorize Princeton University to lend this thesis to other institutions or individuals for the purpose of scholarly research.

I further authorize Princeton University to reproduce this thesis by photocopying or by other means, in total or in part, at the request of other institutions or individuals for the purpose of scholarly research.

Acknowledgments

I would like to express my heartfelt appreciation to my advisor, Professor David P. Billington. In my initial conversation with him, we were discussing possible thesis topics, and he asked me why I had come to Princeton. I wasn't quite sure how to answer the question at the time, but I am sure now. I came for the opportunity to work with quality faculty members like him. People who know that learning is more than what you get from a book, and teaching is more than standing in front of a blackboard. Thanks for the inspiration and patience, Professor!

I am also indebted to my committee members, Professors Robert Mark and Jiann-Wen Ju, who provided equal inspiration through their courses, and who read this thesis and offered their suggestions.

I would also like to thank the Civil Engineer Corps of the U.S. Navy, for allowing me this opportunity. It's not just a job!

A special thank you goes out to the many friends I have met during the year. I wish you continued success. Especially to John Matteo, who helped me in reviewing many projects by providing his keen insight and thoughtful words of wisdom.

Additionally, I would like to thank Captain and Mrs. G, and Jane and Martin, who all introduced me to Princeton and gave me their never ending support.

Finally, I would like to thank my wife, Teri, who stood by me all the way, and put up with the person who possessed my body for the last two weeks of writing this thesis.

Abstract

The debate between Anton Tedesko and Charles S. Whitney which occurred from the 1930's through the 1950's typifies the confusion among designers in the United States regarding thin shell concrete roof design. Each man thought his method was correct and designed structures constructed in America during the first half of the twentieth century. By taking a closer look at their debate, we can gain some insight into their methods of design. To resolve the conflict, we then apply modern methods of analysis to analyze a hangar model Whitney had presented in his articles. A full span analysis is performed using the finite element computer program P-FRAME. In addition, we address concerns which were not incorporated into the original analysis. We employ the methods of Milo S. Ketchum and Robert S. Rowe to compute deflection moments for the structure. In addition, we use Ketchum and Rowe's work as background for developing the Initial Deflection Method of computing buckling safety factors. To validate the procedure, we compute buckling safety factors for a variety of structures and compare them to classical formulations.

Table of Contents

To my Father,
who was always there to give me a push when I needed one,
and to my Mother
who was always there to make sure he didn't push too hard.

Chapter One

Introduction

Over the last century, designers such as Eugene Freyssinet, Robert Maillart, Pierre Luigi Nervi, Felix Candela and Heinz Isler have brought the art of reinforced concrete design to its mature state.

Isler's thin shell concrete roofs cover many European structures. From tennis courts to gas stations, his shells provide practical, yet interesting, solutions to everyday roofing problems.

In the United States, however, reinforced concrete design has not advanced as it has abroad. A reflection of this lack of progress can be seen in the content of basic design texts. During the 1950's, in the well known text book by George Winter and Arthur H. Nilson, Design of Concrete Structures, an entire chapter was dedicated to arch and shell design. In the 1991 edition, the words arch and shell do not even appear in the index.[1] Why has this type of design disappeared from our basic text books?

A possible explanation is that a general confusion exists in America regarding shell behavior and because of this, key safety questions still remain unanswered.

This confusion is clearly demonstrated in the debate between Charles S. Whitney (1902-1961) and Anton Tedesko (b. 1902) which took place in the 1940's and 1950's concerning concrete barrel shell roof design. The design is a thin concrete barrel shaped shell with arch stiffeners spaced along the length. The debate focused on how to position the shell in relation to the arches.

Tedesko's opinion was that the shell should be positioned at the rib extremity. Whitney, on the other hand, believed that the shell should be located

at the mid-height of the rib. They debated in many engineering publications, but without resolution.

Tedesko was an Austrian born engineer who had studied civil engineering at the Technological Institute in Vienna in the early 1920's, and had learned thin-shell concrete roof design while working at the firm of Dyckerhoff and Widmann in Weisbaden. In 1932, because of prior work experience in the U.S., he was sent to work in America when his firm decided to expand its operations.[2] Once there, he gained an affiliation with the Roberts and Schaefer Company in Chicago, and stayed on with them to do extensive thin-shell design work during the 1930's and 40's. Because of his effort in this capacity, he introduced thin-shell concrete roof structures to the United States.[3] Examples of his work are the Ice Hockey Arena in Hershey, Pennsylvania which opened in 1936 and the U.S. Navy Hangars at North Island in San Diego, California designed in 1941.

Whitney was an American born designer who wrote two major articles on arch design in the 1920's. In the 1940's, he developed a new desing method for barrel shell roofs that he called ". . . a novel feature. . . . which has important advantages." [4] In his method, he placed a great emphasis on volume change moments, which are a function of the cross sectional moment of inertia. The moments of inertia would be less if the shell was located in the middle of the rib, thus, this was the better design.

Whitney also designed structures which were constructed in the United States. An example of his work is the Field House at Syracuse University built in the 1950's.

We can see, then, that two very different methods of design existed

simultaneously. The debate between Whitney and Tedesko which started in the literature over 40 years ago, has not been resolved. In this thesis, we will first examine the different design methods and then utilize modern engineering tools to clarify the debate.

We look at Whitney's method by examining calculations which were prepared for a hangar model and presented in articles published during the 1940's and 1950's. Tedesko's rebuttal to one of the articles is also scrutinized to examine his ideas on the subject.

In our modern analysis, we use the finite element method to analyze Whitney's hangar model. Additionally, we employ the methods of Robert S. Rowe and Milo S. Ketchum to calculate stress amplification due to deflections in arches. Using these as a starting point, we develop a method of predicting buckling loads for arched structures.

Chapter Two

Whitney's "New Idea"

Whitney began writing about concrete arch design as early as 1925 with his article, "Design of Symmetrical Concrete Arches" published in the American Society of Civil Engineers (ASCE) Transactions. Between 1932 and 1940 he was the Chairman of the American Concrete Institute (ACI) Committee 312 which was attempting to establish standards for reinforced concrete arch design. His ideas appear in this committee's reports published in 1932 and 1940.

It wasn't until after this that he began writing about his method of concrete barrel shell roof design. He presented his ideas in three articles published between 1943 and 1955.

The structure Whitney analyzes in developing his claims is a 220 foot clear span aircraft hangar model. The hangar roof is a parabolic barrel shell comprised of a 4 inch thick reinforced concrete slab with ribs spaced 20 feet center to center. The rib cross section varies from 18 x 32 inches at the crown to 18 x 40 inches at each springing. The height of the rib center line above the supports at mid-span is 27.5 feet, and the roof is supported at each springing by concrete A-frames. Whitney assumes that the A-frames act to fix the ends of the barrel shell by restricting translational and rotational motion. Figure 1 is a longitudinal and transverse section of Whitney's model. This structure was first presented in his 1944 article "Aircraft Hangars of Reinforced Concrete".[5]

The article that we will focus on was published in the ACI Journal in June

1950 under the title, "Cost of Long Span Concrete Roof Shells". In this article, Whitney explains the advantages of his design method:

> "An important feature of this type of construction is the placing of the shell near the neutral axis of the ribs so that the ribs project about half above and half below the shell. The principal effects of this arrangement structurally are the elimination of edge stresses in the shell due to rib flexure and the reduction of the stiffness of the combined rib and shell with a corresponding reduction in volume change moments." [6]

He also develops a chart which shows how his shell positioning reduces required rib size and thus, construction cost.

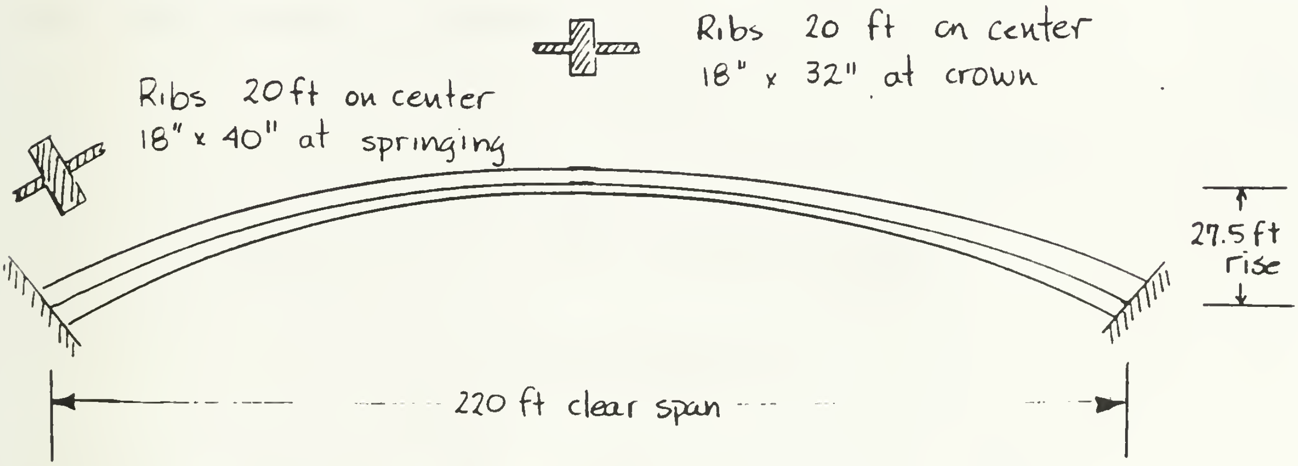

Figure 1. Longitudinal and transverse sections of the 220 ft span hangar model

His chart, shown in Figure 2, presents three different crown cross sections, each based on a 20 foot spacing of the arch ribs. The first cross section has the shell located at the mid-height of the rib, the second has the shell positioned at the top of a similar rib, and the third has the shell at the top of

an enlarged rib. The larger rib in the third cross section is necessary, according to Whitney, to provide the equivalent strength of the first cross section.

To understand Whitney's method of design, we will examine the numbers in his chart. Since Whitney did not publish detailed calculations, we must use information from his other articles and reports to estimate his results.

As his first table entry, Whitney gives the moment of inertia at the crown. For the first section, it is computed using the 20 foot width and including reinforcing steel at the top and bottom of the rib. In the next two sections, he only uses a 14 foot width in his calculations. He explains that with the slab at the top of the rib, only 70% of the shell is effective. Whitney does not provide any background for this assumption in any of his published material, but we can verify it with a formula published in a 1990 textbook on concrete shell design.[7] The effective overhang of one side of the shell, b_e, is:

$$b_e = 0.76\,(r\,h)^{\frac{1}{2}}$$

where: $r = \dfrac{L^2}{8\,d}$ with: $L =$ Span, $d =$ Rise

$h =$ Shell thickness

Using Whitney's data for the hangar model:

$$b_e = 6.5 \text{ ft}$$

This gives a total overhang of 13 ft. When the rib width is considered, the total effective width becomes 14.5 ft, which compares very well with Whitney's 14 ft assumption.

Using Whitney's data at the crown for the hangar model, our computed

moments of inertia for the three cross sections are:

Section 1: 58,000 in^4
Section 2: 117,200 in^4
Section 3: 154,800 in^4

These compare very favorably to Whitney's numbers. Detailed calculations appear in Appendix A.

Arch Cross Sections	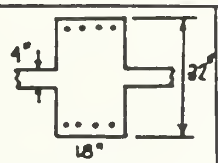	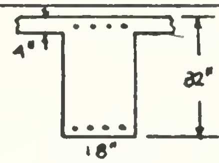	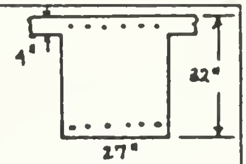
Moment of inertia of crown section	58,000 $in.^4$	116,300 $in.^4$	154,300 $in.^4$
Moment due to live load	1,710,000 in.lb.	1,710,000 in.lb.	1,710,000 in.lb.
Moment due to volume change	1,026,000 in.lb.	2,042,000 in.lb.	2,670,000 in.lb.
Total moment	2,736,000 in.lb.	3,752,000 in.lb.	4,380,000 in.lb.
Maximum horiz-ontal thrust	447,120 lb.	450,170 lb.	508,300 lb.

Figure 2. Whitney's Data Table

The second entry is live load bending moment. Whitney uses 30 psf as the live load for all three cross sections. For a 20 foot width, this results in a distributed load of:

$$30 \text{ psf} \times 20 \text{ ft} = 600 \frac{\text{lb}}{\text{ft}}$$

In his 1925 article, Whitney derives formulas to compute moments in concrete arches for different loads with varying cross sections. From Figure 50 in the 1925 article, the maximum positive live load moment at the crown is:[8]

$$M_l = K_l \; p \; L^2$$

where: p = Uniformly distributed live load
L = Span length in feet
K_l = Factor from Figure 50 using entering arguments N and m

with:

$$N = \frac{y_o}{r} = \frac{\text{quarterpoint rise - midspan rise}}{\text{midspan rise}}$$

$$m = \frac{I_c}{I_s \cos \theta_s} \quad \text{with:} \quad c = \text{crown values}$$

$$s = \text{springing values}$$

Using Whitney's data for the hangar model:

$$m = 0.59 \quad \text{and} \quad N = 0.25$$

With these as entering arguments for table 50:

$$K_l = 0.0049$$

The maximum positive live load moment at the crown is:

$$M_l = 142{,}300 \text{ ft-lb} = 1{,}710{,}000 \text{ in-lb}$$

Whitney presents this value in the table for all three cases. Even though the cross sectional length for the second and third cases is less, he is assuming the effective cross section carries the full live load.

To determine load positioning, Whitney uses influence lines. Figures 35-39 in his 1925 article give influence lines for values of "m" ranging from 0.15 to 0.40 and "N" values ranging from 0.15 to 0.25. From these figures, we can extrapolate the load positioning necessary to produce maximum positive moment at the crown for m = 0.59 and N = 0.25, which is shown in figure 3.

The third value Whitney lists is the volume change moment. The values are based on "rib shortening and a temperature drop of 40 degrees F including the effect of shrinkage."[9]

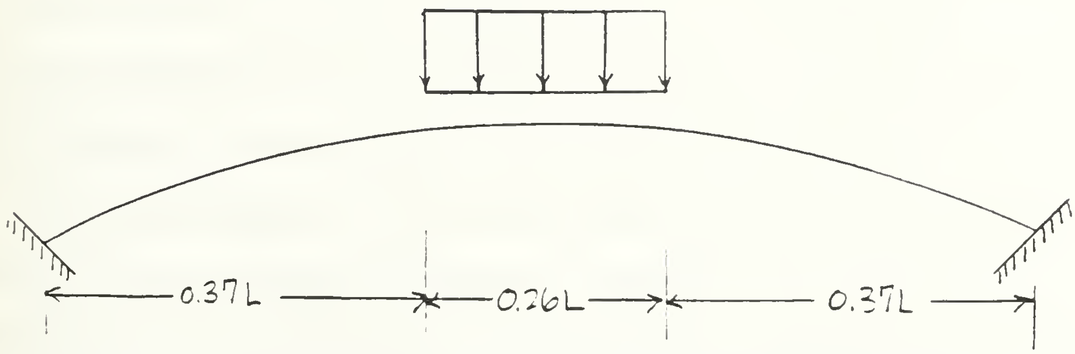

Figure 3. Load distribution to produce maximum positive crown moments

Rib shortening results from compressive axial forces in the structure, and the 40 °F temperature drop accounts for the worst case combination of temperature change and concrete shrinkage. Obviously, shrinkage produces an outward thrust with corresponding negative moments at the supports. With a temperature drop, these two effects would add together and make sense when considered with the 30 psf live load Whitney is using, which is probably a snow load.

In the "Aircraft Hangars of Reinforced Concrete" article, Whitney provides insight to his choice of a 40 °F temperature drop. First of all, he states that because plastic flow reduces temperature and shrinkage effects, 60% of the maximum temperature range for a geographical area should be used for concrete arch calculations. In the article, he presents a table of temperature ranges for various locations in the United States. We will choose a value from

the table for a location in the south, since this is what Whitney implies he used. The temperature range of 95 °F for New Orleans, Louisiana is chosen. The design range is therefore:

$$95\ °F \times 60\% = 57\ °F$$

Assuming that it drops from the mean, our change in temperature will be half of the design range, or 27 °F. Whitney suggests that the stress caused by shrinkage in concrete can also be represented by a drop in temperature. Using his shrinkage value of 15°F results in a total temperature drop 42 °F. [10]

The volume change moments are computed by first calculating the thrusts due to rib shortening and temperature changes. The thrusts are multiplied by a function of the rise to compute moments. Using Whitney's 1925 article, Micalos derives formulas for hingeless (fixed) arches. If we assume a secant variation in the cross section, the formula for computing thrust due to rib shortening is:[11]

$$H_{RS} = \frac{45}{4} \frac{H}{A_m} \frac{I_c}{h^2}$$

where:

I_c = Crown moment of inertia
h = Mid span rise
A_m = Mean rib area
H = Dead and live load thrust

Using Whitney's data, the thrust due to rib shortening is:

$$H_{RS} = 4{,}180 \text{ lb}$$

The thrust due to temperature changes is computed from:[12]

$$H_T = \frac{45}{4} \alpha T E \frac{I_c}{h^2}$$

where: α = Coefficient of thermal expansion
T = Temperature change

Using Whitney's data and his recommended coefficient of thermal expansion of 5.5×10^{-6} in/in/°F, the thrust due to temperature change is:[13]

$$H_t = 5270 \text{ lb}$$

The crown moment due to the total volume change thrust is:

$$M = \frac{1}{3} h \; (H_{RS} + H_t)$$

With Whitney's data, the crown moment due to volume changes is:

$$M = 1{,}039{,}000 \text{ in-lb}$$

This value compares well with Whitney's value of 1,026,000 in-lb. Whitney does not explain his assuming a secant variation in cross section for this calculation.

The table entries for the other two sections vary directly with the moments of inertia. Thus, the volume change moment at the crown is nearly doubled when the shell is shifted from the mid-height to the extremity, and it is increased even more for the larger rib.

The next table entry, the total moment, is simply the addition of the two previously calculated values. Since the live load moment is the same for all three cross sections, the total moment varies only with the change in volume change moments.

Finally, Whitney computes the maximum horizontal thrust caused by the dead and live loads. Whitney's formula for computing thrust due to dead load is:[14]

$$H_d = \frac{w_c \, L_1^2 \, (g - 1)}{r \;\, k^2}$$

where: g = The ratio of springing to crown weight

w_c = Crown weight in lb/ft
L_1 = One-half the span length
$k = \cosh^{-1}(g)$

Using 150 lb/ft^3 as the weight of concrete, the dead load thrust is:

$$H_d = 337{,}600 \text{ lb}$$

The live load thrust for a load that produces the maximum positive moment at the crown is:[15]

$$H_l = \frac{C_l \, p \, L^2}{r}$$

where: C_l = A constant computed from Figure 51using m and N
r = Midspan rise
p = Distributed live load

For Whitney's data:

$$H_l = 62{,}800 \text{ lb}$$

The dead and live load total thrust is:

$$H = 400{,}400 \text{ lb}$$

This value is 46,720 lb lower than the table value of 447,120 lb. Whitney must be considering the full span live load in his calculations. To compute the full span live load thrust, we will use the previously defined formula with a C_l value for both maximum positive and negative crown moment live loads:[16]

$$H_l = 132{,}000 \text{ lb}$$

The total thrust would then be:

$$H = 469{,}600 \text{ lb}$$

This is 22,500 lb higher than the table value. Even if we consider the negative thrust from the volume change calculations, the computed total thrust would still be 13,000 lb higher than the table value. Whitney does not give any explanation for this difference.

In summary, through his table, Whitney shows the importance of volume change moments in concrete barrel shell roof design. According to his conclusions, placing the shell at the mid-height of the rib cuts the volume change moment in half and is the most efficient design. He also claims that with the shell located at the extremity, the rib must be increased by 50% to give the equivalent strength of a cross section with the shell at mid-height. He does not, however, present any calculations to support this claim.

Chapter Three

Tedesko's Design Ideas

Whitney's ideas did not go unchallenged. The discussions of his papers raised serious questions as to the validity of his claims. In presenting the alternate viewpoint, we will focus on two papers in particular. The first is the discussion of Whitney's 1950 paper "Cost of Long-Span Concrete Roof Shells", and the second is the discussion of the 1940 report of ACI Committee 312, "Plain and Reinforced Arches" . Both discussions were written by Structural Engineers from the Roberts and Schaefer Company of New York City, who were under the direction of Anton Tedesko at the time.[17] Therefore, we will consider the alternate viewpoint as Tedesko's.

Tedesko does not agree with Whitney's claim regarding shell position. Tedesko believes, instead, that the shell should be positioned at the rib extremity. He develops an alternate chart which shows that the rib width can be decreased if the shell is moved to the top or bottom. He supports his arguement by looking at the stress distribution and by computing buckling safety factors.

We will examine Tedesko's chart, Figure 4, to gain more insight into his argument. Tedesko uses four crown cross-sections which he calls cases one through four. The first two cross sections are the same as presented in Whitney's table. The third has the shell at the bottom of the 18 inch wide rib, and the fourth has the reduced rib with the shell at the top.

The first five items are the same ones listed by Whitney. Tedesko carries the calculations a bit farther, however, by computing stress distributions, tension force taken by the reinforcing steel and a buckling safety factor.

Arch Cross Sections	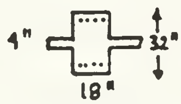 Case 1	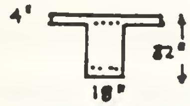 Case 2	 Case 3	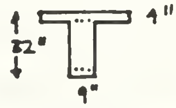 Case 4
Moment of inertia of crown section, in.	58,000	116,300	116,300	69,700
Moment due to live load, in. -lb	1,710,000	1,710,000	1,710,000	1,710,000
Moment due to volume change, in. -lb	1,026,000	2,042,000	2,042,000	1,230,000
Total moment, in. -lb	2,736,000	3,752,000	3,752,000	2,940,000
Max. horizontal thrust. lb	447,120	450,000	450,000	408,000
Concrete stress at top of arch psi	-1,096	-628	-1,091	-696
Concrete stress at bottom or arch, psi	413	404	-59	663
Total tension force in concrete to be taken by reinf., lb	32,500 (min. reinf.- 2.9 sq. in.)	44,500 (min. reinf.- 2.9 sq. in.)	0 (min. reinf.- 2.9 sq. in.)	46,000 (min. reinf.- 2.9 sq. in.)
Relative buckling safety of arch -- proportional to I (Dischinger's method)	8.7	17.4	17.4	10.5

Figure 4. Tedesko's data chart

The moments of inertia for the first two crown sections are the same as Whitney's. Tedesko apparently agrees with Whitney's use of the reduced

effective width when the shell is moved to the rib extremities. The moment of inertia for the third cross section is the same as the second since the two are mirror images. Their only differences will be in the section modulus for the top and bottom fibers, but this will only affect the stress distribution. For the fourth cross section, Tedesko computes the moment of inertia using the full 20 foot width. Since the shell is positioned at the top of the rib, however, the reduced effective width should be 14 feet. Using the reduced effective width, we calculate the moment of inertia to be 65,300 in^4; 4,400in^4 lower than Tedesko's table value.

The moment due to live load is the same as Whitney's and the same for all four cases. Tedesko is not challenging Whitney's use of the full width loading on the reduced effective width, the amount of load used, or his load position.

The moments due to volume changes vary directly with the crown moment of inertia as in Whitney's table, and the values for the first three cross sections are the same as before. Tedesko is not questioning the method of computation. The moment for the fourth case is about 6% too high due to Tedesko's full width moment of inertia. Using Whitney's volume change moment as a starting point, we calculate the moment for the fourth cross section to be 1,147,000 in-lb. This is 83,000 in-lb lower than Tedesko's value.

As in Whitney's table, the total moments are computed directly from the live load and volume change moments. The total for case four using an effective width of 14 ft is 2,857,000 in-lb.

Tedesko's table values for horizontal thrust for the first three cases are the same as Whitney's. He apparently concurs with the calculations from Whitney's 1925 article. The thrust for the fourth cross section is computed using Whitney's formulas as well. We concur with this value as it is not affected by the

change in moment of inertia.

The next data entry in Tedesko's chart is the stress distribution across the crown cross section. This is computed using standard formulas for axial and bending stress and the appropriate section modulus. Tedesko assumes an uncracked cross section, therefore, an elastic analysis is implied. Since the horizontal thrusts are all compressive, and the bending moments at the crown are all positive, general formulas for computing stresses at the extreme fibers are:

top: $$f_t = -\frac{P}{A} - \frac{M}{S_t}$$ bottom: $$f_b = -\frac{P}{A} + \frac{M}{S_b}$$

where:
- $P =$ Horizontal Thrust
- $A =$ Cross sectional Area
- $M =$ Total Bending Moment
- $S =$ Section Modulus (I /y)

Using Whitney's data for the cross section in case one:

$$f_t = -1060 \text{ psi} \qquad \text{and} \qquad f_b = +449 \text{ psi}$$

Tedesko's values are 36 psi lower for both the top and bottom fibers for case one. To arrive at the stresses listed in the table for the first cross section, Tedesko is either using a total thrust value of 499,800 lb instead of the listed value of 447,120 lbs or using a reduced cross sectional area. He does not explain the change. The stress calculations for the other three cases also differ from what would be expected from Whitney's data, but they do show the trend Tedesko wants to demonstrate. In case four, the stresses are almost equally distributed and even with the reduced rib, the stresses are still well within the strength of concrete.

Next, Tedesko lists the total tension force to be taken by the reinforcing

steel. This is calculated assuming a linear stress distribution and assuming the concrete does not carry tension. The first step in computing this value is to determine the distance from the bottom fiber to the neutral axis. This can be done using a ratio of the table stresses and the rib depth:

$$\bar{y}_b = \frac{413 \text{ psi}}{(413 + 1096) \text{ psi}} (32 \text{ in}) = 8.75 \text{ in}$$

From this, the total tensile force is:

$$T = \frac{1}{2} (413\text{psi})(18 \text{ in})(8.75 \text{ in}) = 32{,}500 \text{ lb}$$

This agrees exactly with the table value. With this value for tension, and assuming a yield stress in the steel of 50 ksi, the required reinforcing steel area would be less than one square inch. The ACI code for minimum reinforcing steel area would supersede, thus requiring a reinforcing steel area of:[18]

$$\rho_{min} = 0.005 = \frac{A_s}{b\,d}$$

Solving for A_s using the rib cross section yields:

$$A_s = 0.005\left(576 \text{ in}^2\right) = 2.88 \text{ in}^2$$

This explains the table reference to minimum required reinforcing steel and agrees with Tedesko's recommended steel area. The tension force and required steel areas are calculated similarly for the other cases. For case three, the required tension force is zero since the entire cross section is in compression at the crown.

Tedesko computes a safety factor against buckling as the last table value for each cross section. The computations are based on Dischinger's formula:[19]

$$V_s = \frac{33.21\ E\ I}{H\ a^2}$$

where:

H = Horizontal Thrust
E = Effective Modulus of elasticity
a = One-half the Span Length
I = Moment of Inertia at the Crown

Using the data for the first cross section with Tedesko's thrust value of 499,820 lb yields a buckling safety factor of:

$$V_s = 8.8$$

This value compares very well with the table value of 8.7. The safety factors for the other cross sections are computed using this formula and show how the they are increased when the shell is moved to the rib extremity. Even with the reduced rib in case four, the safety factor against buckling is larger than when the shell is positioned at mid-height.

Using the same hangar model and data as Whitney does, Tedesko has reached the opposite conclusion. In his table, with the shell moved to the rib extremity, the rib size can be reduced. Which conclusion is correct?

Chapter Four

Resolving the Conflict

Our examination thus far reveals questions which must be addressed to resolve the shell positioning conflict. In addition to these, other items which affect the issue are mentioned in the Whitney and Tedesko articles, but are not incorporated into their tables.

First of all, Tedesko states that additional analysis is required:

> ". . . the writers do not believe it justified to assume that an investigation of the crown of the arch alone can determine the most economic cross section. Not only do the maximum moments vary in sign and magnitude along the arch axis, but also the relative importance of the volume change moments varies. In the lower quarters of the arch the volume change moments are only a small percentage of the total design moments."[20]

Although this is a very serious discrepancy, he does not make the full span analysis he claims is necessary.

Secondly, both sides mention arch deformation effects. And although they both imply that the deflections are easily approximated, neither side presents any relative data. Whitney even stresses the importance of investigating the moments caused by deformations, especially at the crown section where "the greatest increase in stress due to deflection occurs."[21] Tedesko gives some justification for not investigating the additional moments:

> ". . . deformation moments are of important influence only for arches of small buckling safety and for arches which do not follow the pressure line for dead load" [22]

He obviously does not consider the deflection moments to be significant in this design.

Also, the two factions address using a reduced Young's Modulus to account for concrete creep when computing deflections. Whitney states that the Young's Modulus value for concrete should be reduced by two-thirds to three-quarters to calculate deflections under permanent load.[23] Tedesko suggests using a value of 2,000,000 psi for E_c to account for creep.[24]

To resolve the question of shell position, we will use an approach that incorporates analysis methods not available to Whitney and Tedesko and addresses the additional points mentioned above. Using the four step process outlined below, we will create a table for each of our three cross sections which we can use to make comparisons between the two design methods. The resulting tables are attached as appendix B.

REVISED FOUR STEP METHOD OF ANALYSIS

Step 1 Computing Forces, Moments and Deflections

We make a full span analysis of the barrel shell roof section utilizing the Finite Element computer Program P-FRAME. From the finite element analysis, we are able to determine dead load moments, positive and negative moments due to different live load distributions, volume change moments due to temperature change, axial thrusts at each section and deflections due to the loadings. We model three different cross sections and create a table for each.

We model the arches using the 20 foot width and 4 inch shell thickness Whitney specified. The first cross section has the shell at the mid-height of the rib and will be referred to as the "Whitney Arch". The second is 14 feet long, has the shell located at the lower rib extremity and will be referred to as the

"Tedesko Arch". Both of these arches have ribs that vary from 18 x 32 at the crown to 18 x 40 at the springing. The third section is 14 foot wide, has a smaller rib and has the shell located at the lower extremity. It will be referred to as the "Reduced Tedesko Arch". We chose to position the shell at the bottom of the rib for the Reduced Tedesko Arch since this will result in a compressive stress distribution through more of the arch span. Since we are designing in concrete, this is an important consideration. The rib for this section varies from 9 x 32 at the crown to 9 x 40 at the springing. The three cross sections are shown in Figure 7.

We used 29 nodes to model each arch, 23 of which are spaced horizontally from zero to 220 feet at equal 10 foot intervals. The other six nodes are placed to allow for the live loads necessary to make a full span analysis. To ensure symmetry, we placed three nodes on each side of the mid-span. Vertical positions for the nodes were computed using the equation for a parabola. A one-line diagram of the model is shown in Figure 5.

The moments of inertia at the crown for the first two arches are taken directly from Whitney's table. We use the corrected moment of inertia from the Tedesko table for the third. Moment of inertia at the springing is computed using Whitney's dimensions. These calculations appear in Appendix A. To represent the varying cross section, we use a linear interpolation between the crown and springing, adjusting the value every 10 feet. The Young's Modulus for all cases is 4×10^6 psi, the same as used by Whitney and Tedesko, and the coefficient of thermal expansion we chose is 5.5×10^{-6} in/in/°F, the value that Whitney recommends. The end restraints for the arches are modeled as fixed against both rotation and translation. For all three cases, we chose a linear elastic

analysis.

To compute dead loads, we input the normal density of concrete, 150 lb/ft^3, and P-FRAME computes the weights based on cross sectional areas and

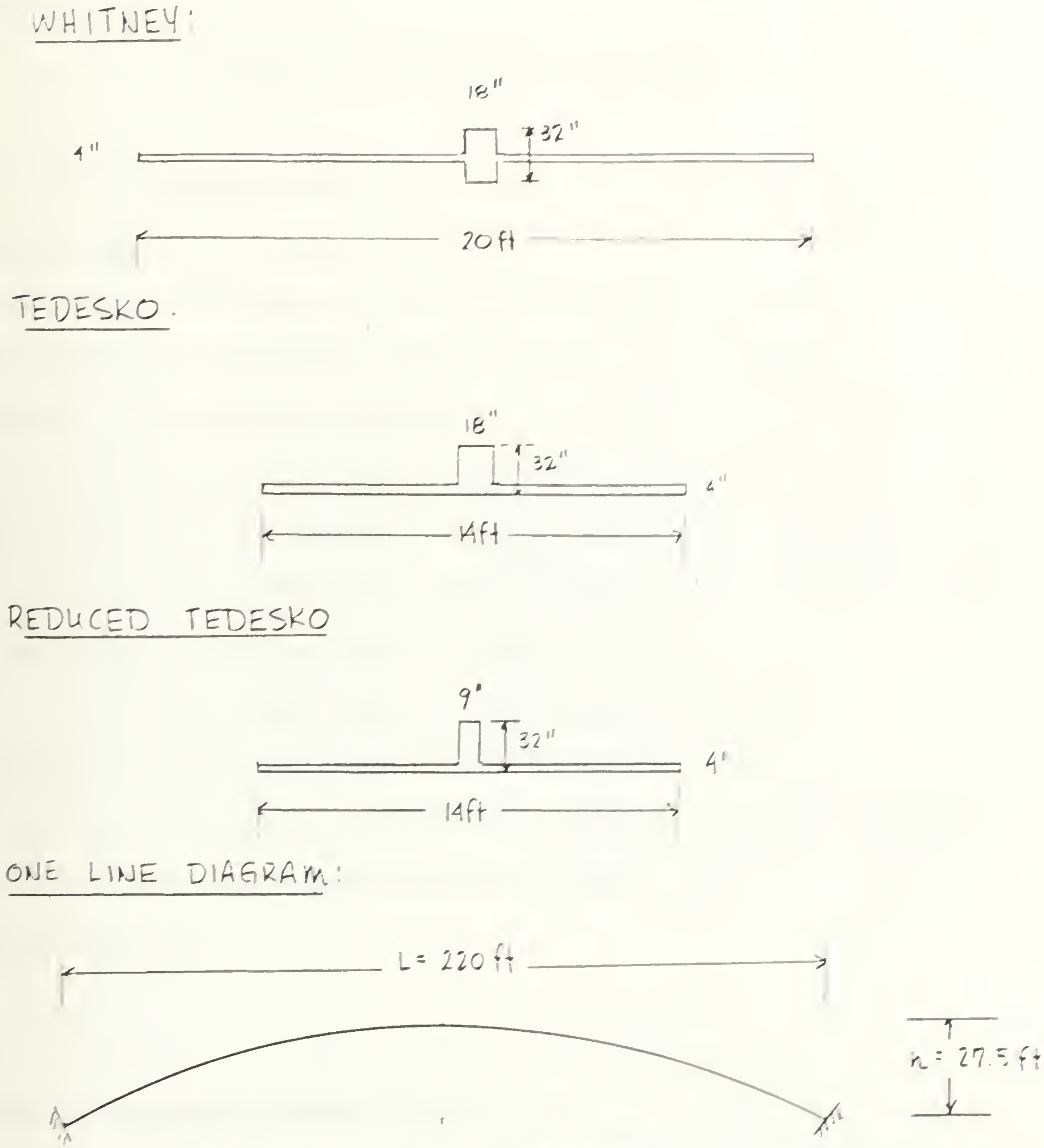

Figure 5. Crown cross sections and One-line diagram for the computer model.

lengths between the nodes. For the Tedesko arches, an additional externally applied dead weight was added to account for the reduced effective width. This was modeled as a uniformly distributed horizontal load. The values for this load were computed as:

$$(20\ \mathrm{ft} - 14\ \mathrm{ft})(4\ \mathrm{in})\left(\frac{1\ \mathrm{ft}}{12\ \mathrm{in}}\right)\left(150\ \frac{\mathrm{lb}}{\mathrm{ft}^3}\right) = 300\ \frac{\mathrm{lb}}{\mathrm{ft}}$$

The live loads are modeled as uniformly distributed and externally applied using Whitney's magnitude of 30 psf. For the full span analysis, we had to load the arch with several different live load distributions to produce maximum positive and negative moments at the points we wanted to investigate. Although data is available through P-FRAME for every nodal point, we concentrated our live load analysis on three significant points; the springing, the quarter point, and the crown. Each arch is loaded using known distributions to produce maximum positive and negative moments at the points of interest.[25] Load distributions used are shown in Figure 6.

To model the volume change moments, we applied a uniform temperature change of -40 °F along the full span of each arch. The rib shortening contribution to the volume change moments is computed directly by P-FRAME. The program determines the axial deformations due to the applied dead and live loads.

Step 2 Computing Deflection Moments

To compute the additional moments due to deflections,we applied the theories of Robert S. Rowe and Milo S. Ketchum to the output data from P-

FRAME. Both of these procedures are based on series approximations of the deflections. To account for the affect of creep, we used a Young's modulus of 2,000,000 psi in the computer analysis.

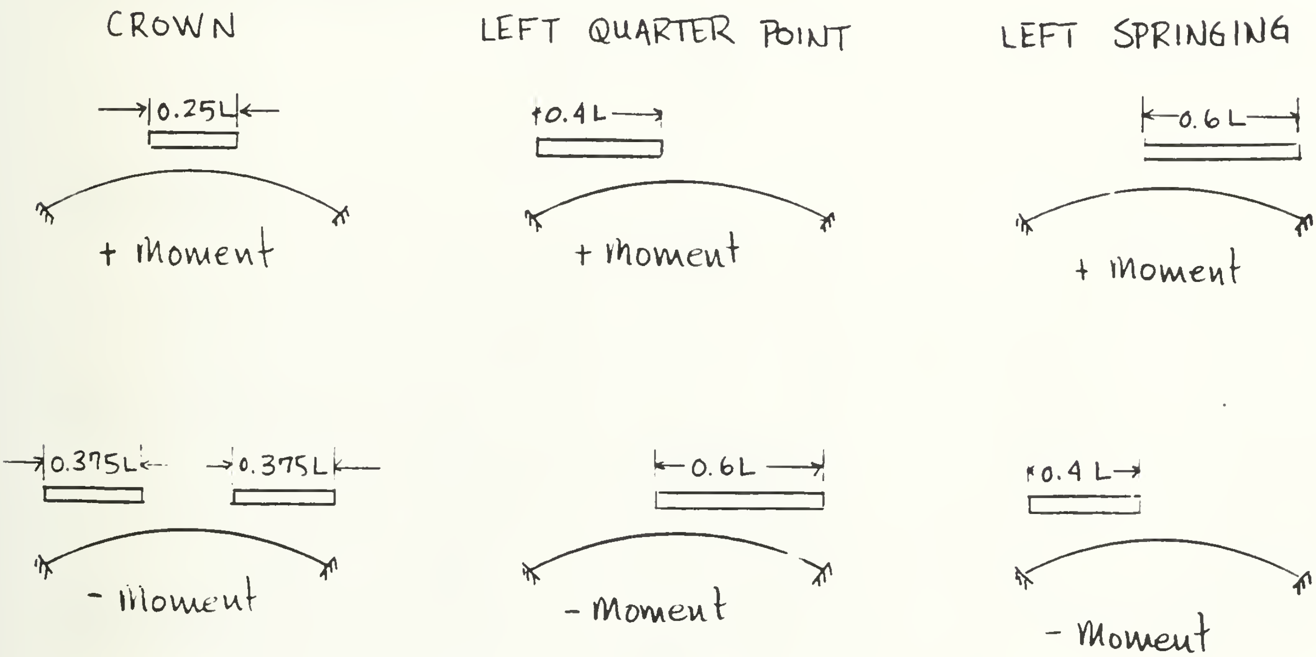

Figure 6. Live load distributions used for Arch analyses

Ketchum's procedure, published in the American Society of Civil Engineers (ASCE) Transactions, provides a method for computing final deflections as a function of initial deflection, moment and axial force.[26] The derivation is based on a beam which is loaded both axially and laterally as shown in Figure 7. In the figure, M_L is the moment due to q, the lateral load, w_i

is the deflection caused by the lateral load, w_a is the deflection due to the axial load and w_o is the total deflection. Relating the deflections:

$$w_o = w_i + w_a$$

Assuming the elastic deflection curves for both loads are similar to their bending moment diagrams, a relationship is established between the ratios of the deflections and moments at the midpoint of the beam:

$$\frac{w_a}{w_i} = \frac{P\,w_o}{M_L}$$

Solving for w_a:

$$w_a = \frac{w_i \quad Pw_o}{M_L}$$

Since $w_a = w_o - w_i$:

$$w_o = w_i + w_i\left(\frac{Pw_o}{M_L}\right)$$

Regrouping:

$$w_o\left(1 - \frac{Pw_i}{M_L}\right) = w_i$$

Solving for w_o:

$$w_o = \frac{w_i}{\left(1 - \frac{Pw_i}{M_L}\right)}$$

Thus, the final deflection, w_o, can be computed if the initial deflection, the axial force and the moment are known. This formula is adapted for our use in computing deflection moments for the tables in appendix B as follows:

$$M_o = \frac{M_i}{\left(1 - \frac{M_i}{M_L}\right)}$$

The deflection moment can be computed if the initial deflection, axial force and moment at a section are known. The initial data (P, w_i, M_L) is available from our computer analysis.

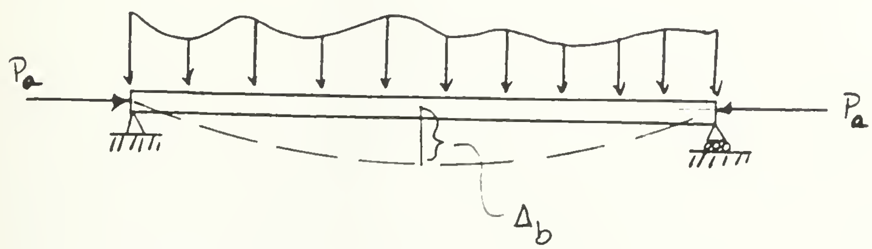

Figure 7. Axially and Laterally loaded beam used in the Ketchum derivation.

Robert S. Rowe's procedure is derrived using a beam loaded both axially and laterally as shown in Figure 8. Rowe's method expanded on Ketchum's work by applying it to arches as well as beams.[27] Rowe's procedure is once again based on the idea of a series of moments. From Figure 8, the deflection, Δb, due to the arbitrary lateral load can be expressed as:

$$\Delta b = (n) \left(\frac{ML^2}{EI}\right)$$

where "n" is a bending moment diagram shape factor.

The moment caused by this deflection and the given axial load is:

$$M_{axail} = P_a \Delta_b$$

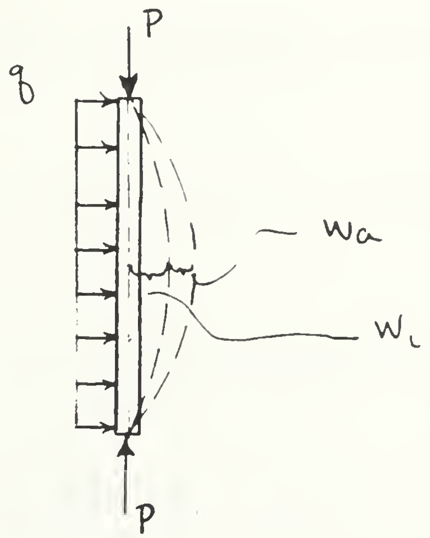

Figure 8. Loaded Beam used in the derivation of Robert S. Rowe's method

This moment causes an additional deflection of:

$$\Delta_{ad} = n_a \left(\frac{M_a L^2}{E\ I} \right) = n_a \left(\frac{P_a \Delta_b L^2}{E\ I} \right)$$

Which, in turn, causes an additional moment:

$$M_a' = P_a\ \Delta_{ad} = P_a \left(n_a \frac{P_a \Delta_b L^2}{E\ I} \right)$$

Assuming the elastic curve maintains the same shape so the n_a's are similar, the total moment equation becomes:

$$M = M_b + P_a \Delta_b + P_a \Delta_b n_a \left(\frac{P_a L^2}{E I} \right) + P_a \Delta_b n_a^2 \left(\frac{P_a L^2}{E I} \right)^2 + \ldots\ldots$$

Since $n_a \left(\frac{P_a L^2}{E I} \right) < 1$, this becomes:

$$M = M_b + P_a \Delta_b \left(1 + n_a \left(\frac{P_a L^2}{E I} \right) + \text{higher order terms which go to zero} \right)$$

Multiplying through by $\left(\frac{1 - A}{1 - A} \right)$ where $A = n_a \frac{P_a L^2}{E I}$:

$$M = \frac{M_b(1 - A) + P_a \Delta_b (1 - A^2)}{1 - A}$$

With $A < 1$, A^2 goes to zero, therefore:

$$M = \frac{M_b(1 - A) + P_a \Delta_b}{1 - A}$$

Assuming the axial load and lateral load bending moment diagrams are similar,

$n_a = n_b$, and since we know $\Delta_b = n_b \frac{M_b L^2}{E I}$, the moment equation becomes:

$$M = \frac{M_b \left(1 - n_a \frac{P_a L^2}{E I} \right) + \left(P_a n_a \frac{M_b L^2}{E I} \right)}{1 - n_a \frac{P_a L^2}{E I}} = \frac{M_b \left(1 + n_a \frac{P_a L^2}{E I} - n_a \frac{P_a L^2}{E I} \right)}{1 - n_a \frac{P_a L^2}{E I}}$$

Therefore:

$$M = \frac{M_b}{1 - n_a \frac{P_a L^2}{E I}}$$

The total bending moment, including the deformation effects, can be computed in terms of the bending moment at the section, the axial load at the section and a bending moment diagram shape factor. This is very similar to Ketchum's final result.

Rowe applies this to curved beams. He presents a chart that relates the displacement ratios in straight and curved beams to the h/L value in the curved beam. From his chart, we see that for arches with rise to span ratios of less than 0.15, the deflection in an arch is less than 2% different from that in a straight beam.[28]

Step 3 Computing Cross Sectional Stresses

Stress distributions are computed using the total moments and axial thrusts at each section and the standard P/A and My/I stress formulas. Results from these calculations appear in each of the tables.

Step 4 Computing Buckling Safety Factors

A revised method of computing buckling safety factors, based on the theories of Rowe and Ketchum, is presented in the following chapter. Data for each arch is presented at the end of this chapter.

EXPLANATION OF TABULAR DATA

General

We show a full span analysis in the three tables in appendix B. Data is computed for the crown, the left and right springing and the left and right quarter points. The data is displayed in columns from left to right along the arch length. An explanation of each line, along with a sample calculation for the "Whitney Arch" follows. The P-FRAME output file for the Whitney Arch is attached as Appendix C.

Moment of Inertia, Line (A)

Moments of inertia for the first two tables are computed based on Whitney's data for the crown and springing rib sizes. The quarter point value is linearly interpolated. Data for the third table is calculated based on Tedesko's reduced rib width, using Whitney's variation in rib height .

For Whitney's Arch, the moment of inertia at the crown was previously computed as $58{,}000 \text{ in}^4$. For the given rib dimensions of 18 x 40 at the springing, the moment of inertia is $110{,}000 \text{ in}^4$. Using a linear interpolation between the two to compute the quarter point value yields $84{,}000 \text{ in}^4$.

Moments due to dead and live load, Line (B)

These values are taken from P-FRAME output for the cross sections with positive moments acting clockwise at the left and counter-clockwise at the right hand end of a segment. The dead load is calculated based on a linear interpolation of cross section variation every 10 feet. Dead load for the full 20

foot width is applied for all three arches. Load positions for moments due to live loads are shown for the four cases in Figure 8. P-FRAME data is converted from ft-kips to in-lb for easy comparison with Whitney and Tedesko data and is rounded to four places. For the Whitney Arch at the crown (node 15):

Moment due to dead load	= -30.20 ft-kips	= -363,000 in-lb
Moment due to live load (1), (Maximum positive crown Moment)	= +136.4 ft-kips	= +1,636,000 in-lb
Moment due to live load (2), (Maximum negative crown Moment)	= -133.7 ft-kips	= -1,604,000 in-lb
Moment due to live load (3), (Maximum positive moment at the Left Quarter Point or Maximum negative moment at the Left Springing)	= -64.48 ft-kips	= -774,000 in-lb
Moment due to live load (4) (Maximum negative moment at the Left Quarter Point or Maximum positive moment at the Left Springing)	= +67.10 ft-kips	= +805,000 in-lb

Initial Displacements, Line (C)

These values are also taken from P-FRAME output and represent displacement of the nodal points from their initial positions due to the indicated loads. The displacements shown are in inches and do not include deformation moment effects. The dead load displacements are computed using E = 2,000,000 psi to account for creep. For Whitney's Arch at the crown:

Initial Displacement due to Dead Load	= -0.345 inches
Initial Displacement due to Live Load case (1)	= -0.541 inches
Initial Displacement due to Live Load case (2)	= +0.419 inches
Initial Displacement due to Live Load case (3)	= +0.180 inches

Initial Displacement due to Live Load case (4) = -0.302 inches

Axial Thrusts, Line (D)

Once again, the Values are taken directly from P-FRAME output. The thrusts are normal to the indicated cross section and are listed in kips. For Whitney's Arch at the crown:

Axial thrust for Dead Load = 351.6 kips
Axial thrust for Live load Case (1) = 60.6 kips
Axial thrust for Live load Case (2) = 70.6 kips
Axial thrust for Live load Case (3) = 41.1 kips
Axial thrust for Live load Case (4) = 90.1 kips

This would give a total thrust of 412,200 lb for dead plus live load for maximum positive moment at the crown, and a thrust of 482,800 lb for dead plus full span live load. These values are 3% higher than the thrusts of 400,400 lb and 469,600 lb computed using Whitney's formulas.

Temperature Change Moments, Line (E)

These moments are computed based on the 40°F temperature drop used by Whitney applied over the entire arch. The rib shortening contribution, computed by Whitney for his volume change moments, is not included here since it is computed as part of the Load Moment in line (B). The P-FRAME output is once again adjusted from ft-kips to in-lb for comparison with Whitney and Tedesko table values. For the crown section of Whitney's Arch:

Temperature Change Moment = 59.87 ft-kips = 718,000 in-lb

.

If our computed values of dead load, live load for maximum moment at

the crown, and temperature change moments are added together, we can make a comparison with the total moment value listed in Whitney's table. The P-FRAME total moment would be 1,991,000 in-lb. This is 27% lower than Whitney's table value of 2,736,000 in-lb.

Moments due to Deflection, Line (F)

As the h/L value for our arch is 0.125, according to Rowe, we can compute the deflection moments using Ketchum's method. We use P-FRAME output to compute the axial thrust, initial deflection and moment at the section for each live load condition. The dead and temperature change loads will not create deflection moments since they are uniformly distributed across the entire arch span. The arch axis will not deflect from the funnicular line under these two loads.

For Whitney's Arch at the crown, the deflection moment at the crown due to live load case (1) is computed using:

$$M = \frac{P\, w_i}{\left(1 - \frac{P\, w_i}{M_L}\right)}$$

From P-RFRAME output
for Live load case (1) : $P =$ 60,600 lbs (compression)
$w_i =$ -0.541 in
$M_L =$ 1,636,000 in-lb

The deflection moment at the crown for live load case (1) is:

$$M = +\ 33{,}000 \text{ in-lbs}$$

The moment sign is determined by the orientation of the deflection and axial force. In this case, the arch is deflecting downward, and the axial force is

compressive, thus, a positive moment results.

Worst Case Moments (G)

The worst case moments are totaled from Lines B, E and F for dead and live loads. The live load case which produces the largest appropriate moment is used in each computation. A circled number appears next to the worst case moment value to indicate which live load was used. For the crown section of Whitney's Arch:

Worst case total Moment = +2,024,000 in-lb

The worst case total moment for the crown results from a live load for maximum positive moment.

Section Stress, Line (H)

Stresses are calculated based on worst case moments and associated axial loads. Standard stress formulas are used with the computed cross sectional areas and section moduli for the appropriate point in the arch. For the crown section of Whitney's Arch:

Axial Load for Worst case Total Moment = 412,200 lb (compression)

Top and bottom fiber stresses:

$$f_t = -840 \text{ psi} \qquad \text{and} \qquad f_b = +277 \text{ psi}$$

Buckling Safety Factor

A safety factor against buckling is computed based on the Initial Deflection Method for arches developed in Chapter 5. First, models of the

Whitney Arch, the Tedesko Arch and the Reduced Tedesko Arch are given a parabolic imperfection. We determine the critical load using the Initial Deflection Method, and compute a buckling safety factor by comparing the critical load to the dead load plus the 600 lb/ft live load used by Whitney. The finite element analysis program P-FRAME is used to compute the initial deflections.

For each arch, the initial imperfection is a parabola with a midspan rise of 0.625 ft. We compute the revised nodal coordinates using the transformation described in Chapter 5. The revised coordinates are input to the P-FRAME program, and we apply a uniformly distributed horizontal load across the entire span. To compute the critical load, we must eliminate the rib shortening contribution. A purely parabolic model of the arch is loaded with the same uniform load, and the resulting deflections are subtracted from those computed using the offset model. The final deflections are due to bending moment only. The critical load occurs when the deflection is equal to the offset.

For Whitney's Arch, at a uniform load of 23.5 kips/ft, the deflections for the offset model at the three-quarter point (node 23) are:

$$\delta_{x23} = -0.224 \text{ in} \qquad \text{and} \qquad \delta_{y23} = -2.49 \text{ in}$$

The deflections for the parabolic model are:

$$\delta_{x23} = -2.76 \text{ in} \qquad \text{and} \qquad \delta_{y23} = -9.56 \text{ in}$$

This results in a total deflection of:

$$\delta = -7.51 \text{ in} = -0.625 \text{ ft}$$

To compute the buckling safety factor, we assume a uniformly distributed dead load equal to the average cross sectional value. The buckling safety factor for Whitney's arch is:

Safety Factor = 23.5 /2.2 = 10.7

The P-FRAME input and putput used in this calculation are attached as appendix D. Using the Initial Deflection Method for the other two arches yields critical loads of:

Tedesko Arch	=	47.5 kips/ft
Reduced Tedesko Arch	=	27.2 kips/ft

The resulting Buckling Safety Factors are:

Tedesko Arch	=	25.0
Reduced Tedesko Arch	=	17.4

These values are higher than the Dischinger values listed in Tedesko's table, but show the same trend. Even with a reduced rib, the Tedesko cross section has a greater safety against buckling than Whitney's.

Chapter Five

The Initial Deflection Method For Computing Critical Buckling Loads

Using the ideas of Rowe and Ketchum, we will develop a relationship between successive deflections and buckling. The general formula is developed using an axially loaded column.

An axially loaded column which is perfectly straight theoretically will not buckle, regardless of the applied load. It will only deform along its axis in accordance with the well known formula:

$$\delta_a = \frac{PL}{AE}$$

where:

P = Axially applied load
L = Column length
A = Cross sectional area
E = Young's modulus

Given some type of initial imperfection, however, the column will buckle under sufficient load. For the axially loaded column shown in Figure 11 that has an initial parabolic offset with a value of δ_o at mid-height, the initial moment at the mid-span is:

$$M_o = P\,\delta_o$$

This moment , in turn, causes an additional deflection, δ_1:

$$\delta_1 = \frac{M_o L^2}{12\,E\,I} = \frac{(P\,\delta_o)\,L^2}{12\,E\,I}$$

Letting $B = \dfrac{P L^2}{12 E I}$, the additional moment due to the deflection δ_1 is:

$$M_1 = P \delta_1 = P \delta_0 B$$

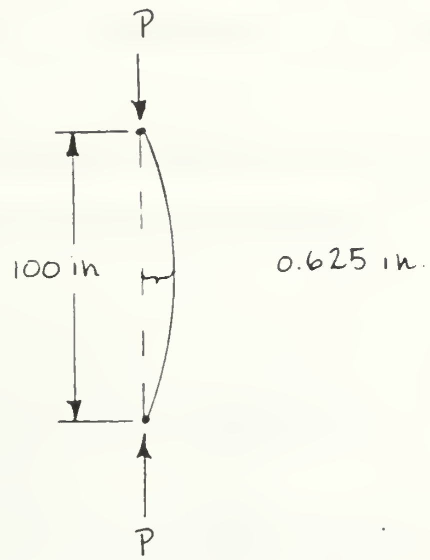

Figure 9. Axially loaded column with initial parabolic offset

This moment will create an additional deflection , δ_2:

$$\delta_2 = \frac{M_1 L^2}{12 E I} = \delta_0 B^2$$

The total moment is:

$$M_T = M_0 + M_1 + M_2 + \ldots = P \delta_0 + P \delta_1 + P \delta_2 + \ldots = P \delta_0 \left(1 + B + B^2 + \ldots\right)$$

Thus, if B is greater than one, the series diverges, the moments will grow without bound, and the column will buckle. The critical load occurs when B = 1. When B = 1, the original offset, δ_0, and the initial deflection, δ_1, will be related as:

$$\delta_1 = B\,\delta_0 = \delta_0$$

We have defined the critical point in terms of deflection. When the initial deflection is equal to the original offset, the column is at the critical point. If the initial deflection is greater than the original offset, the column will buckle. This criteria is easily applied to output from finite element computer programs. To check buckling, one only needs to compare the computer generated deflections to chosen input imperfections.

As a check, we will compare the results from the "Initial Deflection Method" with several well known buckling formulations.

Euler Column Buckling

We will check the initial deflection buckling criteria against the classic buckling problem presented by Euler. His solution for the critical load of a column hinged at both ends is: [29]

$$P_{cr} = \pi^2 \frac{E\,I}{L^2}$$

where:

P = Column axial load
L = Length between the supports
E = Young's Modulus
I = Minimum moment of inertia of the cross section

The physical model used is a 100 inch long steel beam with a 12 square inch cross section which is 6" x 2 ". The beam is hinged at both ends.

Since the chosen cross section results in a minimum moment of inertia of 4 in^4, the critical load using Euler's formula is:

$$P_{cr} = 118 \text{ kips}$$

To test the Initial Deflection Method, the beam is modeled on the finite element computer program SAP-90 using frame elements with 11 equally spaced vertical nodes. The horizontal offset for each node is calculated using a parabolic equation with the chosen maximum offset as 0.625 inches at the mid-span. The column is modeled with a pin at the bottom and a roller at the top. Loads are applied in the negative vertical direction at the top node. The critical load is one that produces a 0.625 inch deflection at the middle node. To determine the critical point, we start at the theoretical critical load and perform iterations until we read a deflection of 0.625 inches on the output.

Using the Initial Deflection Method with SAP-90, the critical load is :

$$P_{cr} = 116 \text{ kips}$$

This is 1.7% lower than Euler's theoretical value.

Plate Buckling

Next, we check the initial deflection buckling criteria against the theory for a simply supported plate. The physical structure we model is a 100 inch by 100 inch steel plate which is one inch thick.

The general formula for critical load per length for a simply supported plate uniformly compressed in one direction is:[30]

$$(N_x)_{cr} = \frac{\pi^2 D}{b^2} \left(\frac{b}{a} + \frac{a}{b}\right)^2$$

where:

a = Horizontal plate dimension
b = Vertical plate dimension
N_x = Load per unit length along the horizontal

and: $$D = \frac{E\,h^3}{12\left(1 - \nu^2\right)}$$

where:
E = Young's modulus
h = Plate thickness
ν = Poisson's ratio

For a square plate, a = b, and this becomes:

$$(N_x)_{cr} = \frac{4\,\pi^2 D}{a^2}$$

For the chosen plate, with $E = 30 \times 10^6$ psi and $\nu = 0.3$, the flexural rigidity is:

$$D = 2{,}747 \text{ in-kips}$$

From the Timoshenko formula, the critical distributed load is:

$$(N_x)_{cr} = 1084 \ \frac{\text{kips}}{\text{in}}$$

The structure is modeled using the finite element computer program SAP-90 with 100 plate elements. The computer model is composed of 121 nodes with 11 nodes spaced equally along the horizontal, and 11 vertical nodes equally spaced at each of these. Each vertical line of nodes has a parabolic offset with a maximum of 0.625 inches at the middle node. The plate is simply supported on all sides with a pin along the bottom edge and rollers along the other three. We model the uniform load across the top of the plate as a pressure load.

As with the axially loaded column, the critical loading occurs when the mid-span horizontal deflection equals the original offset. Using this criteria, we load the plate at the theoretical critical load, and adjust as necessary until we see a mid-span deflection of 0.625 inches in the computer output.

Using the Initial Deflection Method, the critical load is:

$$(N_x)_{cr} = 911 \ \frac{\text{kips}}{\text{in}}$$

This result is 15.6 % lower than the theoretical buckling load. This result is suprising in light of the success with the column data.

Arch Buckling

In a two hinged parabolic arch, uniformly distributed loads are carried axially to the supports. Bending moments are zero throughout, and the arch simply "squats" due to rib shortening. By introducing an initial imperfection as we did with the axially loaded column, however, bending moments are created (Figure 12 refers). The moments can be expressed as:

$$M_o = P\,\delta_o$$

where: P = Axial load at the section
δ_o = initial offset from the funicular line

The greatest moments will occur at the points where the largest offset is located. These bending moments will, in turn, cause additional deflections. These deflections are expressed as they were for the axially loaded column as:

$$\delta_1 = \frac{M_o L^2}{12\,E\,I} = \frac{(P\,\delta_o)\,L^2}{12\,E\,I}$$

Using the same derivation as in the case of the axially loaded column, we can define the critical point of arch buckling in terms of deflection. When the initial deflection is equal to the original offset, the arch is critically loaded. If the initial deflection is greater than the original offset, the arch will buckle. To compute buckling loads using the Initial Deflection Method, we need to compare computer generated deflections to our chosen offsets.

To validate the Initial Deflection Method for arch buckling, we will compare it with Timoshenko's theoretical results. The model we use is a 2 hinged steel arch with a constant 6" x 2" cross section. The arch spans 100 inches horizontally and has a rise of 10 inches.

Timoshenko's general formula to compute critical loads for a uniformly loaded parabolic arch with a constant cross section is:[31]

$$q_{cr} = \lambda_4 \frac{EI}{L^3}$$

where:

E = Young's modulus
I = Moment of inertia
L = Horizontal span length
λ_4 = A factor depending on the height to span ratio and the number of hinges

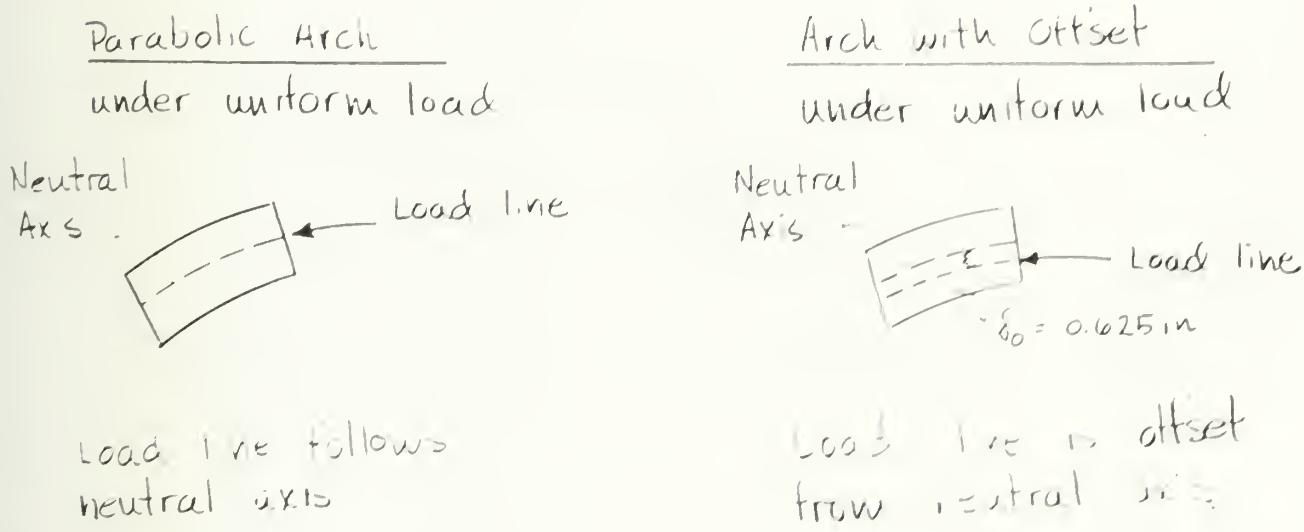

Figure 10. Bending Moments in Arches caused by Initial Offset

From Timoshenko's Table 7-5 with h/L = 0.1, $\lambda_4 = 28.5$. The critical load with $E = 30 \times 10^6$ is:

$$q_{cr} = 3.42 \text{ kips per inch of horizontal span}$$

The Initial Deflection Method is tested using the finite element computer program P-FRAME. We model the arch using 21 nodes equally spaced along the horizontal and compute initial vertical coordinates for these nodes using a parabolic equation with a rise of 10 inches at the middle node. The arch is free to rotate and restricted from translating at both ends.

We will apply a parabolic offset to each half span as shown in Figure 11.

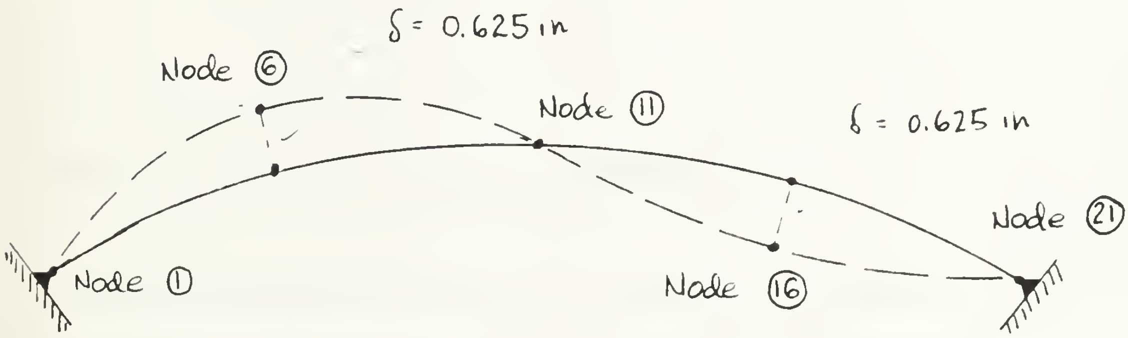

Figure 11. Parabolic Offset used in the Computer Model

The maximum offset will be 0.625 inches at each quarter point. Since we want the nodes to be offset from the initial parabolic curve, each node will have to be adjusted both vertically and horizontally as shown for node 5 in Figure 12. The

change in coordinates will be a function of the parabolic offset, δ_5, and the angle θ_5 as:

$$\delta_{y5} = \delta_5(\cos\theta_5) \qquad \text{and} \qquad \delta_{x5} = \delta_5(\sin\theta_5)$$

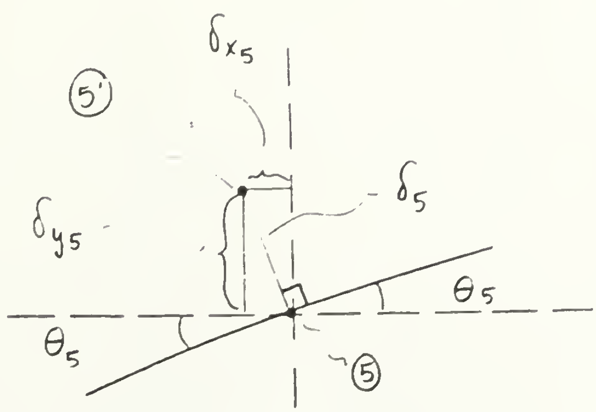

Figure 12. Blown up view of the coordinate transformation at node 5

The arch is loaded using uniformly distributed horizontal loads. To eliminate the affect of rib shortening from the computer output, a purely parabolic arch model without initial offsets is loaded with a uniformly distributed critical load. The rib shortening deflections are subtracted from the deflections computed using the offset model. The resulting deflections are due to bending moment only. Once again, the theoretical buckling load is chosen as a starting point and iterations are performed until we see an adjusted deflection of 0.625 in either half of the arch. Using the Initial Deflection Method, the buckling load for the arch model is:

$$P_{CR} = 2.92 \frac{\text{kips}}{\text{in}}$$

This is 14.6% lower than Timoshenko's theoretical value of 3.42 kips/in.

Chapter Six

Conclusions

From the debate between Charles S. Whitney and Anton Tedesko we can draw several conclusions. First of all, Whitney's 1925 article was a good guideline for arch design. His formulas and charts give information which is backed up by modern methods of analysis. Using only graphic statics and the Calculus, he computed formulas and charts to determine thrusts and moments for significant loads and load positions at several points in the arch. For maximum positive moment at the crown, his distribution is less than 1% different from accepted design guidelines used from the 1950's to today. His adjustment factors allow quick computations for a very diverse range of arch designs. Although his conclusions for thin shell design are vehemently challenged by Tedesko, his method of calculating arch thrusts, live load moments and volume change moments are not.

Secondly, Tedesko's claim that a full span analysis is necessary for arch design is valid. By looking at our full span analysis, we can see that stress distributions at the springing, quarter point and crown must all be investigated. The crown analysis that Whitney and Tedesko both present is not sufficient to design a barrel shell roof.

Next, both men were correct in their claim that the deflection moments are not significant for Whitney's hangar model at the assumed live loads. We can see, however, that the deflection moments and corresponding stresses must be addressed in barrel shell roof design. As the factor of safety against buckling is reduced, the deflection moments become more significant. The

methods of Rowe and Ketchum are a reliable way to determine deflection moments from data available from most finite element programs.

Additionally, Whitney's emphasis on volume change moments is valid. His claim that the shell should be located at the mid-height of the rib to reduce volume change moments is also valid. There is an irrefuteable relationship between the moment of inertia and the volume change moment. When we look at stress distributions over the full span and take all loads into account, however, we see that the decreased moment of inertia has a drawback. Reducing the moment of inertia increases the tensile stresses near the supports. The tensile stress at the springing for Whitney's Arch is double that of Tedesko's Arch.

Also, there is a significant advantage in placing the shell at the bottom of the rib as opposed to the top. Because concrete is weak in tension and strong in compression, we want to reduce tensile stresses as much as possible. Placing the shell at the bottom of the rib does this. We can see from the stress distributions for Tedesko's Arch and Tedesko's Reduced Arch that tension only exists in upper part of the cross section for the first and last quarter of the arch.

The Initial Deflection Method is a tool which can be used with existing finite element computer programs to compute buckling safety factors for a variety of structures. Although longhand computations of initial offset values are tedious, this could easily be written into a finite element computer program. The critical loads computed with the Initial Deflection Method are conservative for plates, but could provide a ready check for buckling capacity for arches during an iterative design process.

End Notes

[1]George Winter and Arthur H. Nilson, Design of Concrete Structures, Eighth and Eleventh Editions, (New York: McGraw Hill, 1958 and 1991)

[2]David P. Billington, "Anton Tedesko: Thin Shells and Esthetics", Journal of the Structural Division, Proceedings of the American Society of Civil Engineers, Vol 109, No. ST11 (November 1982), p. 2544.

[3]Ibid, p. 2539.

[4]Charles S. Whitney, "Aircraft Hangars and Teminal Buildings of Reinforced Concrete" Aeronautical Engineering Review, Vol 3, (September 1944), p. 39.

[5] Ibid., p. 41.

[6] Charles S. Whitney, "Cost of Long Span Concrete Roof Shells", Journal of the American Concrete Institute, Vol 21, (June 1950), p. 766.

[7]David P. Billington, Thin Shell Concrete Structures, (New York: McGraw-Hill, 1990), p. 212.

[8]Charles S. Whitney, "Design of Symmetrical Concrete Arches", Transactions of the American Society of Civil Engineers, (1925), p. 947.

[9]Whitney, "Cost of Long Span Concrete Roof Shells", p. 767.

[10]Charles S. Whitney, "Aircraft Hangars of Reinforced Concrete", Modern Developments in Reinforced Concrete, No. 7, (Portland Cement Association, 1943), p. 14.

[11]James Micalos, Theory of Structural Analysis and Design, (New York: The Ronald Press Company, 1958), p.307.

[12] Ibid, p. 305.

[13]Whitney, "Aircraft Hangars of Reinforced Concrete", p. 14.

[14]Whitney, "Design of Symmetrical Concrete Arches", p. 972.

[15]Ibid., p. 1026.

[16]Ibid.

[17]Conversation with David P. Billington, Professor, Princeton University, Princeton, New Jersey, 20 June, 1991.

[18]George Winter and Arthur H. Nilson, Design of Concrete Structures, Tenth Edition, (New York: McGraw Hill, 1986), p. 100.

[19]Anton Tedesko et al., "Discussion of a Paper by Charles S. Whitney: Cost of Long Span Concrete Shell Roofs" Journal of the American Concrete Institute, (June 1950), p. 766-3.

[20]Ibid, p. 766-2.

[21]Whitney, "Aircraft Hangars of Reinforced Concrete", p. 14.

[22]Anton Tedesko et al., "Discussion of a report of Committee 312: Plain and Reinforced Concrete Arches", Journal of the American Concrete Institute, V 47, (May 1951), p. 692-4.

[23]Whitney, "Aircraft Hangars of Reinforced Concrete", p. 13.

[24]Tedesko, "Discussion of a Report of Committee 312", p. 692-3.

[25]Winter and Nilson, Eighth Edition, (1958), p. 451.

[26]Milo S. Ketchum, "Ketchum on Deflections and Moments", Transactions of the American Society of Civil Engineers, (1937), p. 1193.

[27]Robert S. Rowe, "Amplification of Stress in Flexible Steel Arches", Transactions of the American Society of Civil Engineers, (1953), p. 910.

[28]Ibid., p. 922.

29Alexander Chajes, Pricipals of Structural Stability Theory, (Englewood

Cliffs, New Jersey: Prentice-Hall, Inc., 1974), pp. 4-14.

[30]Stephen P. Timoshenko and James M. Gere, Theory of Elastic Stability, Second Edition, (New York: McGraw Hill, 1961), pp. 351-355.

[31]Ibid, p. 303.

References

1. Billington, David P. "Anton Tedesko: Thin Shells and Esthetics", Journal of the Structural Division, Proceedings of the American Society of Civil Engineers, November 1982.

2. Billington, David P. Thin Shell Concrete Structures, New York: McGraw-Hill, 1990.

3. Chajes, Alexander. Pricipals of Structural Stability Theory, Englewood Cliffs, New Jersey: Prentice-Hall, 1974.

4. Gere, James M., and Timoshenko, Stephen P. Theory of Elastic Stability, Second Edition, New York: McGraw Hill, 1961.

5. Hunter, Iain Scott. "Computational Form Finding for Concrete Shell Roofs", Dissertation, Princeton University, 1990.

6. Isler,Heinz. "The Stability of Thin Concrete Shells", Paper presented at the Proceedings of a State-of-the-Art Colloqium, New York, 1982.

7. Ketchum, Milo S. "Ketchum on Deflections and Moments", Transactions of the American Society of Civil Engineers, 1937.

8. Micalos, James. Theory of Structural Analysis and Design, New York: The Ronald Press Company, 1958.

9. Nilson, Arthur H. and Winter, George. Design of Concrete Structures, Eighth, Tenth and Eleventh Editions, New York: McGraw Hill 1958, 1986 and 1991.

10. Rowe, Robert S. "Amplification of Stress in Flexible Steel Arches", Transactions of the American Society of Civil Engineers, 1953.

11. Tedesko, Anton, et al., "Discussion of a report of Committee 312: Plain and Reinforced Concrete Arches", Journal of the American Concrete Institute, May 1951.

12. Tedesko, Anton, et al., "Discussion of a Paper by Charles S. Whitney: Cost of Long Span Concrete Shell Roofs", Journal of the American Concrete Institute, June 1950.

13. Whitney, Charles S. "Design of Symmetrical Concrete Arches", Transactions of the American Society of Civil Engineers, 1925.

14. Whitney, Charles S. "Aircraft Hangars of Reinforced Concrete", Modern Developments in Reinforced Concrete, Portland Cement Association, 1943.

15. Whitney, Charles S. "Aircraft Hangars and Teminal Buildings of Reinforced Concrete" Aeronautical Engineering Review, September 1944.

16. Whitney, Charles S. "Cost of Long Span Concrete Roof Shells", Journal of the American Concrete Institute, June 1950.

17. Whitney, Charles S. "Plain and Reinforced Concrete Arches", Progress Report of Committee 312, Journal of the American Concrete Institute, March 1932.

18. Whitney, Charles S. "Plain and Reinforced Concrete Arches", Progress Report of Committee 312, Journal of the American Concrete Institute, September 1940.

APPENDICIES

Moment of Inertia Calculations

Section 1: 18" thick rib with shell located at mid-height

As = As' = 3.0 inches, n = 7

	I_o	A	y_t	Ay_t	d to na	Ad^2
Rib	49,200	576	16	9220	0	0
Left Shell	592	444	16	7100	0	0
Right Shell	592	444	16	7100	0	0
Top Steel	2	21	2.5	53	13.5	3830
Bottom Steel	2	21	29.5	620	13.5	3830

y = 16.0 in $I = 58{,}000\ in^4$

Section 2: 18" thick rib with shell located at top (Flange 70% effective)

As = As' = 3.0 inches, n = 7

	I_o	A	y_t	Ay_t	d to na	Ad^2
Rib and Steel	56,800	618	16	9890	6.9	29,400
Left Shell	400	300	2	600	7.1	15,100
Right Shell	400	300	2	600	7.1	15,100

y = 9.1 in $I = 117{,}200\ in^4$

Section 3: 27" thick rib with shell located at top (Flange 70% effective)

As = As' = 4.5 inches, n = 7

	I_o	A	y_t	Ay_t	d to na	Ad^2
Rib	73,700	864	16	13,800	5.3	24,300
Left Shell	376	282	2	564	8.7	21,300
Right Shell	376	282	2	564	8.7	21,300
Top Steel	3	32	2.5	80	8.2	2,150
Bottom Steel	3	32	29.5	944	18.8	11,300

y = 10.7 in $I = 154{,}800\ in^4$

Section 2: 9" thick rib with shell located at top (Flange 70% effective)

As = As' = 1.5 inches, n = 7

	I_o	A	y_t	Ay_t	d to na	Ad^2
Rib	24,580	288	16	4608	9.6	26,740
Left Shell	450	318	30	9540	4.4	6160
Right Shell	450	318	30	9540	4.4	6160
Top Steel	0	1.5	2	3	21.6	700
Bottom Steel	0	1.5	30	15	4.4	30

y = 25.6 in $I = 65{,}300\ in^4$

Whitney Arch

	Left Springing	Left Qtr Pt	Crown	Right Qtr Pt	Right Springing
A) Moment of Inertia (in4)	110,000	84,000	58,000	84,000	110,000
B) Load Moment ($x10^6$ in-lb)					
Dead Load	-1.936	+0.321	-0.363	+0.321	-1.936
Live Load 1	+2.575	-1.535	+1.636	-1.535	+2.576
Live Load 2	-2.812	+1.492	-1.604	+1.492	-2.812
Live Load 3	-6.572	+2.996	-0.774	-1.686	+4.159
Live Load 4	+6.335	-3.010	+0.805	+1.643	-4.396
C) Initial Displacements (in)					
Dead Load	0	-0.476	-0.345	-0.476	0
Live Load 1	0	+0.196	-0.541	+0.196	0
Live Load 2	0	-0.260	+0.491	-0.259	0
Live Load 3	0	+1.155	+0.180	-0.917	0
Live Load 4	0	+1.092	-0.302	+0.980	0
D) Axial Thrust (kips)					
Dead Load	397.4	362.3	351.6	362.3	397.4
Live Load 1	61.8	62.8	60.6	62.8	61.8
Live Load 2	85.0	72.5	70.6	72.5	85.0
Live Load 3	56.8	42.9	41.1	41.2	39.7
Live Load 4	89.9	92.4	90.1	94.0	107.1
E) Temperature Change Moment ($x10^6$ in-lb)	-1.774	+0.096	+0.718	+0.096	-1.774
F) Deflection Moments					
Live Load 1	0	-0.012	+0.033	-0.012	0
Live Load 2	0	+0.019	-0.030	+0.019	0
Live Load 3	0	+0.050	-0.007	-0.039	0
Live Load 4	0	-0.104	+0.028	+0.098	0
G) Worst Case Total Moment ($x10^6$ in-lb)	-10.38 (3)	+3.433(3)	+2.024(1)	+2.158(4)	-8.106(4)
H)Section Stress (psi)					
Top	+1593	-996	-840	-755	+1168
Bottom	-2144	+475	+277	+169	-1780

Tedesko Arch

	Left Springing	Left Qtr Pt	Crown	Right Qtr Pt	Right Springing
A) Moment of Inertia (in4)	218,400	167,400	116,300	167,400	218,400
B) Load Moment ($x10^6$ in-lb)					
Dead Load	-2.354	+0.268	+0.002	+0.268	-2.354
Live Load 1	+2.459	-1.527	+1.687	-1.527	-2.459
Live Load 2	-2.941	+1.497	-1.555	+1.497	+2.941
Live Load 3	-6.643	+2.972	-0.744	-1.685	+4.080
Live Load 4	+6.160	-3.002	+0.876	+1.655	-4.562
C) Initial Displacements (in)					
Dead Load	0	-0.474	-0.663	-0.474	0
Live Load 1	0	+0.078	-0.309	+0.078	0
Live Load 2	0	-0.155	+0.165	-0.155	0
Live Load 3	0	-0.595	+0.064	+0.446	0
Live Load 4	0	+0.518	-0.208	-0.524	0
D) Axial Thrust (kips)					
Dead Load	400.5	365.5	354.5	365.5	400.5
Live Load 1	61.3	62.3	60.1	62.3	61.3
Live Load 2	84.5	71.9	70.0	71.9	84.5
Live Load 3	56.6	42.6	40.7	40.9	39.4
Live Load 4	89.3	91.7	89.4	93.3	106.4
E) Temperature Change Moment ($x10^6$ in-lb)	-3.506	+0.193	+1.424	+0.193	-3.506
F) Deflection Moments					
Live Load 1	0	-0.005	+0.019	-0.005	0
Live Load 2	0	+0.011	-0.012	+0.011	0
Live Load 3	0	+0.026	-0.003	-0.018	0
Live Load 4	0	-0.048	+0.019	+0.050	0
G) Worst Case Total Moment ($x10^6$ in-lb)	-12.50 (3)	+3.481(3)	+3.132(1)	+2.166(4)	-9.939(4)
H)Section Stress (psi)					
Top	+1261	-844	-958	-684	+897
Bottom	-1028	-96	-95	-219	-923

Reduced Tedesko Arch

	Left Springing	Left Qtr Pt	Crown	Right Qtr Pt	Right Springing
A) Moment of Inertia (in4)	123,800	94,600	65,300	94,600	123,800
B) Load Moment ($x10^6$ in-lb)					
Dead Load	-1.506	+0.135	+0.001	+0.135	-1.505
Live Load 1	+2.509	-1.532	+1.663	-1.532	-2.509
Live Load 2	-2.891	+1.496	-1.573	+1.496	+2.891
Live Load 3	-6.617	+2.970	-0.755	-1.684	+4.113
Live Load 4	+6.235	-3.005	+0.846	+1.649	-4.495
C) Initial Displacements (in)					
Dead Load	0	-0.507	-0.715	-0.507	0
Live Load 1	0	+0.153	-0.520	+0.153	0
Live Load 2	0	-0.256	+0.325	-0.256	0
Live Load 3	0	-1.041	+0.132	+0.800	0
Live Load 4	0	+0.938	-0.327	-0.903	0
D) Axial Thrust (kips)					
Dead Load	318.9	291.7	282.9	291.7	318.9
Live Load 1	61.5	62.5	60.3	62.5	61.5
Live Load 2	84.7	72.2	70.2	72.1	84.7
Live Load 3	56.7	42.7	40.9	41.0	39.6
Live Load 4	89.5	92.0	89.7	93.6	106.7
E) Temperature Change Moment ($x10^6$ in-lb)	-1.989	+0.107	+0.805	+0.107	-1.989
F) Deflection Moments					
Live Load 1	0	-0.010	+0.032	-0.010	0
Live Load 2	0	+0.019	-0.023	+0.019	0
Live Load 3	0	+0.045	-0.005	-0.033	0
Live Load 4	0	-0.089	+0.030	+0.089	0
G) Worst Case Total Moment ($x10^6$ in-lb)	-10.11 (3)	+3.257(3)	+2.501(1)	+1.980(4)	-7.989(4)
H) Section Stress (psi)					
Top	+2189	-1355	-1350	-1001	+1600
Bottom	-1074	-94	-126	-245	-978

INPUT DATA

WHITNEY'S ARCH

*** JOINT DATA ***

X - coord. (feet)	Y - coord. (feet)	X - Degree of Freedom	Y - Degree of Freedom	Z - Degree of Freedom
0	0	0	0	0
[illegible]	[illegible]	[illegible]	[illegible]	[illegible]

Degree of Freedom: 0=restrained 1=free j=coupled to joint 'j'

*** MEMBER CONNECTIVITY DATA ***

Lower Joint	Greater Joint	Section Number	Material Number	Lower End Type	Greater End Type	Attribute Type	Length (ft)
1	2	1	1	1	1	1	11.0815
2	3	2	1	1	1	1	10.8920
3	4	3	1	1	1	1	10.7220
4	5	4	1	1	1	1	10.5654
5	6	5	1	1	1	1	10.4260
6	7	6	1	1	1	1	5.1688
7	8	7	1	1	1	1	5.1397
8	9	8	1	1	1	1	10.2080
9	10	9	1	1	1	1	10.1256
10	11	10	1	1	1	1	5.5204
11	12	11	1	1	1	1	5.5546
12	13	12	1	1	1	1	5.0090
13	14	13	1	1	1	1	10.0238
14	15	14	1	1	1	1	10.0024
15	16	14	1	1	1	1	10.0024
16	17	13	1	1	1	1	10.0238
17	18	12	1	1	1	1	5.0090
18	19	11	1	1	1	1	5.5548
19	20	10	1	1	1	1	5.5204
20	21	9	1	1	1	1	10.1256
21	22	8	1	1	1	1	10.2080
22	23	7	1	1	1	1	5.1397
23	24	6	1	1	1	1	5.1688
24	25	5	1	1	1	1	10.4260
25	26	4	1	1	1	1	10.5654
26	27	3	1	1	1	1	10.7220
27	28	2	1	1	1	1	10.8920
28	29	1	1	1	1	1	11.0815

:
mber End Types: 1=fixed (rigid connection), 0=pinned (pinned connection).
tribute Type 0 indicates that the member has been deleted.

INPUT DATA

WHITNEY'S ARCH

*** MATERIAL PROPERTY DATA ***

ial r	Youngmod (ksi)	Shearmod (ksi)	Density (K/ft3)	Coeff Exp (/F*1.E-6)	Fy Yield (ksi)
	4000	0	.15	5.5	5

astic Modulus (Young's Modulus) is mandatory.
r non-zero Shear Modulus and Shear Area, secondary deflections due to
ear are included (linear elastic analysis only).
n-zero density is required if self-weight is specified and member weight
to be considered (linear elastic and plastic analysis).
n-zero Thermal Coefficient of Expansion is required for thermal loads.
inear elastic and plastic analysis).
n-zero Yield Stress is mandatory for plastic analysis.

INPUT DATA

WHITNEY'S ARCH

*** SECTION PROPERTY DATA ***

x-sectional Area (in2)	Mom. Inertia (in4)	Shear Area (in2)	Section Mod (in3)	Plastic Moment Capacity (K-ft)
1650	110000	0	0	0
1631	104600	0	0	0
1613	97600	0	0	0
1594	94400	0	0	0
1576	87200	0	0	0
1557	84000	0	0	0
1538	78800	0	0	0
1520	73600	0	0	0
1501	68400	0	0	0
1483	63200	0	0	0
1464	58000	0	0	0

n-zero Cross-sectional Area and Moment of inertia are mandatory.
r non-zero Shear Area, shear stresses are calculated.
r non-zero Shear Area and Shear Modulus, secondary deflections due to
ear are included (linear elastic analysis only).
r non-zero Elastic Section Modulus (S), stresses are calculated.
n-zero Plastic Moment Capacity is mandatory for plastic analysis.

< Printer Banner Goes Here >

DEAD LOAD ANALYSIS (CREEP INCLUDED)

WHITNEY'S ARCH

*** JOINT DISPLACEMENTS ***

Case Results

Joint Number	Load Case	X-Displ. (in)	Y-Displ. (in)	Rotation (rad)
1	1	0.00000	0.00000	0.00000
2	1	.01014	-.05803	-.00075
3	1	.04336	-.17393	-.00101
4	1	.07516	-.29795	-.00093
5	1	.09403	-.39915	-.00066
6	1	.09709	-.46095	-.00030
7	1	.09363	-.47630	-.00016
8	1	.08797	-.48344	-.00003
9	1	.07100	-.47179	.00025
10	1	.05050	-.43344	.00040
11	1	.04545	-.42195	.00039
12	1	.03436	-.39805	.00035
13	1	.03126	-.39019	.00032
14	1	.01470	-.35775	.00021
15	1	0.00000	-.34532	0.00000
16	1	-.01470	-.35775	-.00021
17	1	-.03126	-.39019	-.00032
18	1	-.03456	-.39805	-.00035
19	1	-.04543	-.42198	-.00039
20	1	-.05050	-.43344	-.00040
21	1	-.07100	-.47179	-.00025
22	1	-.08797	-.48344	.00003
23	1	-.09363	-.47630	.00016
24	1	-.09709	-.46095	.00030
25	1	-.09403	-.39915	.00066

RAME Linear Elastic analysis results Str No. C

ELLEY 05 Sep 91 1:08 p

DEAD LOAD ANALYSIS (CREEP INCLUDED)

WHITNEY'S ARCH

Case Results

Joint Number	Load Case	X-Displ. (in)	Y-Displ. (in)	Rotation (rad)
26	1	-.07516	-.29795	.00093
27	1	-.04336	-.17393	.00101
28	1	-.01014	-.05803	.00075
29	1	0.00000	0.00000	0.00000

Printer Banner Goes Here

DEAD LOAD ANALYSIS (CREEP INCLUDED)

WHITNEY'S ARCH

*** MEMBER FORCES ***

Case Results

oad ase	Axial @ LJ (kips)	Shear @ LJ (kips)	BM @ LJ (K-ft)	Axial @ GJ (kips)	Shear @ GJ (kips)	BM @ GJ (K-ft)
1	397.422	16.132	161.355	-389.215	1.056	-77.822
1	388.975	13.714	77.822	-381.641	3.276	-20.976
1	381.484	11.400	20.976	-374.985	5.403	11.174
1	374.857	9.765	-11.174	-369.235	6.842	26.605
1	369.199	8.583	-26.605	-364.356	7.833	30.514
1	364.425	3.326	-30.514	-362.300	4.783	26.748
1	362.316	3.401	-26.748	-360.386	4.709	23.387
1	360.356	6.628	-23.387	-357.071	9.393	9.270
1	357.136	6.507	-9.270	-354.618	9.326	-5.003
1	354.738	1.447	5.003	-354.237	2.462	-6.282
1	354.234	2.871	6.282	-353.265	5.729	-14.190
1	353.311	.467	14.190	-353.014	2.660	-16.392
1	352.765	6.437	16.392	-351.899	8.991	-29.093
1	351.934	7.515	29.093	-351.598	7.735	-30.195
1	351.598	7.735	30.195	-351.934	7.515	-29.093
1	351.899	8.991	29.093	-352.765	6.437	-16.392
1	353.014	2.660	16.392	-353.311	.467	-14.190
1	353.265	5.729	14.190	-354.234	2.871	-6.282
1	354.237	2.462	6.282	-354.738	1.447	-5.003
1	354.618	9.326	5.003	-357.136	6.507	9.270
1	357.071	9.393	-9.270	-360.356	6.628	23.387
1	360.386	4.709	-23.387	-362.316	3.401	26.748
1	362.300	4.783	-26.748	-364.425	3.326	30.514
1	364.356	7.833	-30.514	-369.199	8.583	26.605
1	369.235	6.842	-26.605	-374.857	9.763	11.174

AME Linear Elastic analysis results Str No. 0

LLEY 05 Sep 91 12:53 p

< Printer Banner Goes Here >

DEAD LOAD ANALYSIS (CREEP INCLUDED)

WHITNEY'S ARCH

Case Results

oad ase	Axial @ LJ (kips)	Shear @ LJ (kips)	BM @ LJ (K-ft)	Axial @ GJ (kips)	Shear @ GJ (kips)	BM @ GJ (K-ft)
1	374.985	5.403	-11.174	-361.484	11.400	-20.976
1	381.641	3.276	20.976	-368.975	13.714	-77.822
1	389.215	1.056	77.822	-397.422	16.132	-161.355

AME Linear Elastic analysis results Str No. (

LLEY 05 Sep 91 12:53 p

Printer Banner Goes Here

DEAD LOAD ANALYSIS (CREEP INCLUDED)

WHITNEY'S ARCH

*** SUPPORT REACTIONS ***

Case Results

Joint Number	Load Case	X-Reaction (kips)	Y-Reaction (kips)	Z-Reaction (K-ft)
1	1	351.683	185.805	161.355
29	1	-351.683	185.805	-161.355

AME Linear Elastic analysis results | Str No. 0

LLEY | 05 Sep 91 12:52 p

< Printer Banner Goes Here >

TEMPERATURE LOAD OF 40 DEGREES F

WHITNEY'S ARCH

*** JOINT DISPLACEMENTS ***

Case Results

Joint Number	Load Case	X-Displ. (in)	Y-Displ. (in)	Rotation (rad)
1	1	0.00000	0.00000	0.00000
2	1	-.01216	-.04211	-.00047
3	1	-.00425	-.13263	-.00083
4	1	.01417	-.25833	-.00108
5	1	.03546	-.40673	-.00123
6	1	.05392	-.56608	-.00128
7	1	.06093	-.64642	-.00128
8	1	.06586	-.72540	-.00125
9	1	.06906	-.87446	-.00113
10	1	.06271	-1.00385	-.00094
11	1	.05966	-1.03209	-.00088
12	1	.05126	-1.08738	-.00074
13	1	.04764	-1.10490	-.00068
14	1	.02576	-1.17004	-.00037
15	1	0.00000	-1.19272	0.00000
16	1	-.02576	-1.17004	.00037
17	1	-.04764	-1.10490	.00068
18	1	-.05126	-1.08738	.00074
19	1	-.05966	-1.03209	.00088
20	1	-.06271	-1.00385	.00094
21	1	-.06906	-.87446	.00113
22	1	-.06586	-.72540	.00125
23	1	-.06093	-.64642	.00128
24	[illegible]	-.05392	-.56608	.00128
25	1	-.03546	-.40673	.00123

AME Linear Elastic analysis results Str No. 0

LLEY 05 Sep 91 1:00 p

Printer Banner Goes Here

TEMPERATURE LOAD OF 40 DEGREES F

WHITNEY'S ARCH

Case Results

Joint Number	Load Case	X-Displ. (in)	Y-Displ. (in)	Rotation (rad)
26	1	-.01417	-.25833	.00108
27	1	.00425	-.13263	.00083
28	1	.01216	-.04211	.00047
29	1	0.00000	0.00000	0.00000

< Printer Banner Goes Here

TEMPERATURE LOAD OF 40 DEGREES F

WHITNEY'S ARCH

*** MEMBER FORCES ***

Case Results oad ase	Axial @ LJ (kips)	Shear @ LJ (kips)	BM @ LJ (K-ft)	Axial @ GJ (kips)	Shear @ GJ (kips)	BM @ GJ (K-ft)
1	-6.818	3.255	147.892	6.818	-3.255	-111.816
1	-6.936	2.994	111.816	6.936	-2.994	-79.201
1	-7.046	2.726	79.201	7.046	-2.726	-49.978
1	-7.151	2.438	49.978	7.151	-2.438	-24.215
1	-7.246	2.138	24.215	7.246	-2.138	-1.928
1	-7.308	1.915	1.928	7.308	-1.915	7.969
1	-7.350	1.749	-7.969	7.350	-1.749	16.960
1	-7.401	1.517	-16.960	7.401	-1.517	32.447
1	-7.461	1.186	-32.447	7.461	-1.186	44.460
1	-7.494	.959	-44.460	7.494	-.959	46.878
1	-7.508	.846	-46.878	7.508	-.846	51.562
1	-7.521	.715	-51.562	7.521	-.715	52.997
1	-7.537	.520	-52.997	7.537	-.520	58.210
1	-7.553	.166	-58.210	7.553	-.166	59.872
1	-7.553	-.166	-59.872	7.553	.166	58.210
1	-7.537	-.520	-58.210	7.537	.520	52.997
1	-7.521	-.715	-52.997	7.521	.715	51.562
1	-7.508	-.846	-51.562	7.508	.846	46.878
1	-7.494	-.959	-46.878	7.494	.959	44.460
1	-7.461	-1.186	-44.460	7.461	1.186	32.447
1	-7.401	-1.517	-32.447	7.401	1.517	16.960
1	-7.350	-1.749	-16.960	7.350	1.749	7.969
1	-7.308	-1.915	-7.969	7.308	1.915	-1.928
1	-7.246	-2.138	1.928	7.246	2.138	-24.215
1	-7.151	-2.438	24.215	7.151	2.438	-49.978

AME Linear Elastic analysis results Str No. 0

LLEY 05 Sep 91 1:00 p

< Printer Banner Goes Here >

TEMPERATURE LOAD OF 40 DEGREES F

WHITNEY'S ARCH

ase Results

ad se	Axial @ LJ (kips)	Shear @ LJ (kips)	BM @ LJ (K-ft)	Axial @ GJ (kips)	Shear @ GJ (kips)	BM @ GJ (K-ft)
1	-7.046	-2.726	49.978	7.046	2.726	-79.201
1	-6.936	-2.994	79.201	6.936	2.994	-111.816
1	-6.818	-3.255	111.816	6.818	3.255	-147.892

TEMPERATURE LOAD OF 40 DEGREES F

WHITNEY'S ARCH

*** SUPPORT REACTIONS ***

Case Results

Joint Number	Load Case	X-Reaction (kips)	Y-Reaction (kips)	Z-Reaction (K-ft)
1	1	-7.555	0.000	147.892
29	1	7.555	0.000	-147.892

CHECK OF MOMENTS FOR VARIOUS LOADINGS
WHITNEY 220 FT SPAN ARCH

*** MEMBER LOAD DATA ***

case 1 - member distributed loads

Mem No.	Sloped UDL K/ft slope	Proj. UDL K/ft horiz	Local UDL k/ft perp	Local UDL K/ft parll	Triangular K/ft @ GJ	Thermal Change (F)
11	0	-.6	0	0	0	0
12	0	-.6	0	0	0	0
13	0	-.6	0	0	0	0
14	0	-.6	0	0	0	0
15	0	-.6	0	0	0	0
16	0	-.6	0	0	0	0
17	0	-.6	0	0	0	0
18	0	-.6	0	0	0	0

case 2 - member distributed loads

Mem No.	Sloped UDL K/ft slope	Proj. UDL K/ft horiz	Local UDL k/ft perp	Local UDL K/ft parll	Triangular K/ft @ GJ	Thermal Change (F)
1	0	-.6	0	0	0	0
2	0	-.6	0	0	0	0
3	0	-.6	0	0	0	0
4	0	-.6	0	0	0	0
5	0	-.6	0	0	0	0
6	0	-.6	0	0	0	0
7	0	-.6	0	0	0	0
8	0	-.6	0	0	0	0
9	0	-.6	0	0	0	0
10	0	-.6	0	0	0	0
19	0	-.6	0	0	0	0
20	0	-.6	0	0	0	0
21	0	-.6	0	0	0	0
22	0	-.6	0	0	0	0
23	0	-.6	0	0	0	0
24	0	-.6	0	0	0	0
25	0	-.6	0	0	0	0
26	0	-.6	0	0	0	0
27	0	-.6	0	0	0	0
28	0	-.6	0	0	0	0

case 3 - member distributed loads

Mem No.	Sloped UDL K/ft slope	Proj. UDL K/ft horiz	Local UDL k/ft perp	Local UDL K/ft parll	Triangular K/ft @ GJ	Thermal Change (F)
1	0	-.6	0	0	0	0
2	0	-.6	0	0	0	0
3	0	-.6	0	0	0	0
4	0	-.6	0	0	0	0
5	0	-.6	0	0	0	0
6	0	-.6	0	0	0	0
7	0	-.6	0	0	0	0
8	0	-.6	0	0	0	0
9	0	-.6	0	0	0	0
10	0	-.6	0	0	0	0

CHECK OF MOMENTS FOR VARIOUS LOADINGS
WHITNEY 220 FT SPAN ARCH

_case 3 - member distributed loads

Mem No.	Sloped UDL K/ft slope	Proj. UDL K/ft horiz	Local UDl k/ft perp	Local UDL K/ft parll	Triangular K/ft @ GJ	Thermal Change (F)
11	0	-.6	0	0	0	0

case 4 - member distributed loads

Mem No.	Sloped UDl K/ft slope	Proj. UDL K/ft horiz	Local UDL k/ft perp	Local UDL K/ft parll	Triangular K/ft @ GJ	Thermal Change (F)
12	0	-.6	0	0	0	0
13	0	-.6	0	0	0	0
14	0	-.6	0	0	0	0
15	0	-.6	0	0	0	0
16	0	-.6	0	0	0	0
17	0	-.6	0	0	0	0
18	0	-.6	0	0	0	0
19	0	-.6	0	0	0	0
20	0	-.6	0	0	0	0
21	0	-.6	0	0	0	0
22	0	-.6	0	0	0	0
23	0	-.6	0	0	0	0
24	0	-.6	0	0	0	0
25	0	-.6	0	0	0	0
26	0	-.6	0	0	0	0
27	0	-.6	0	0	0	0
28	0	-.6	0	0	0	0

es:
loped UDL, Projected UDL & Point Loads act in the global coordinate system.
ocal Perpendicular, Local Parallel, Triangular Loads act in
he local member coordinate system.
riangular Loads are 0 at the lower joint with the magnitude specified at
he greater joint.

< Printer Banner Goes Here >

LIVE LOAD ANALYSIS (4 LOAD CASES)

WHITNEY'S ARCH

*** MEMBER FORCES ***

Case Results

oad ase	Axial @ LJ (kips)	Shear @ LJ (kips)	BM @ LJ (K-ft)	Axial @ GJ (kips)	Shear @ GJ (kips)	BM @ GJ (K-ft)
1	61.793	-11.222	-214.662	-61.793	11.222	90.309
2	85.031	14.252	234.363	-82.445	-8.837	-106.434
3	56.686	24.149	547.655	-54.302	-18.735	-310.045
4	89.936	-21.119	-527.955	-89.936	21.119	293.920
1	62.174	-8.869	-90.309	-62.174	8.869	-6.291
2	82.051	11.957	106.434	-79.672	-6.451	-6.174
3	53.552	20.782	310.045	-51.174	-15.273	-113.690
4	90.673	-17.691	-293.920	-90.673	17.691	101.225
1	62.469	-6.472	6.291	-62.469	6.472	-75.682
2	79.366	9.509	6.174	-77.201	-3.913	65.781
3	50.549	17.227	113.690	-48.384	-11.633	41.043
4	91.286	-14.192	-101.225	-91.286	14.192	-50.945
1	62.680	-3.941	75.682	-62.680	3.941	-117.320
2	76.980	7.061	-65.781	-75.043	-1.352	110.066
3	47.575	13.580	-41.043	-45.938	-7.901	154.522
4	91.785	-10.490	50.945	-91.785	10.490	-161.775
1	62.790	-1.320	117.320	-62.790	1.320	-131.082
2	74.921	4.485	-110.066	-73.224	1.270	126.824
3	45.568	9.813	-154.522	-43.870	-4.058	226.829
4	92.143	-6.648	161.775	-92.143	6.648	-231.087
1	62.801	.603	131.082	-62.801	-.603	-127.965
2	73.228	.972	-126.824	-72.468	1.930	124.350
3	43.726	5.399	-226.829	-42.965	-2.497	247.235
4	92.303	-3.824	231.087	-92.303	3.824	-250.851
1	62.771	2.021	127.965	-62.771	-2.021	-117.576
2	72.493	-.273	-124.350	-71.798	3.211	115.347
3	42.898	3.467	-247.235	-42.203	-.548	257.553
4	92.366	-1.738	250.851	-92.366	1.738	-259.783
1	62.677	3.994	117.576	-62.677	-3.994	-76.801
2	71.864	-.951	-115.347	-70.659	4.829	75.636
3	42.165	1.875	-257.553	-40.960	4.002	246.697
4	92.375	1.168	259.783	-92.375	-1.168	-247.862
1	62.437	6.780	76.801	-62.437	-6.780	-8.151
2	70.893	-3.678	-75.636	-69.951	7.603	8.396
3	41.098	-2.176	-246.697	-40.156	8.101	194.667
4	92.282	5.278	247.862	-92.282	-5.278	-194.422
1	62.202	8.673	8.151	-62.202	-8.673	13.708
2	70.210	-7.475	-8.396	-70.020	8.962	-12.318
3	40.383	-6.878	-194.667	-40.193	8.366	175.457
4	92.029	8.076	194.422	-92.029	-8.076	-174.067

AME Linear Elastic analysis results Str No. (

LLEY 05 Sep 91 1:25 p

< Printer Banner Goes Here >

LIVE LOAD ANALYSIS (4 LOAD CASES)

WHITNEY'S ARCH

Case Results

Load Case	Axial @ LJ (kips)	Shear @ LJ (kips)	BM @ LJ (K-ft)	Axial @ GJ (kips)	Shear @ GJ (kips)	BM @ GJ (K-ft)
1	62.064	9.608	-13.708	-61.695	-6.329	57.812
2	70.146	-7.907	12.318	-70.146	7.907	-56.084
3	40.314	-7.760	-175.457	-39.944	11.039	123.432
4	91.897	9.461	174.067	-91.897	-9.461	-121.704
1	61.574	7.410	-57.812	-61.461	-6.215	71.499
2	70.274	-6.676	56.084	-70.274	6.676	-69.496
3	40.132	-10.337	-123.432	-40.132	10.337	102.665
4	91.717	11.071	121.704	-91.603	-9.876	-100.663
1	61.280	7.800	-71.499	-60.867	-1.814	119.686
2	70.423	-4.859	69.496	-70.423	4.859	-118.204
3	40.385	-9.297	-102.665	-40.385	9.297	9.473
4	91.318	12.238	100.663	-90.905	-6.252	-7.990
1	60.715	4.666	-119.686	-60.583	1.333	136.355
2	70.574	-1.553	118.204	-70.574	1.553	-133.734
3	40.777	-7.394	-9.473	-40.777	7.394	-64.483
4	90.512	10.507	7.990	-90.380	-4.508	67.104
1	60.583	1.333	-136.355	-60.715	4.666	119.686
2	70.574	1.553	133.734	-70.574	-1.553	-118.204
3	41.063	-5.593	64.483	-41.063	5.593	-120.430
4	90.094	8.479	-67.104	-90.226	-2.480	121.913
1	60.867	-1.814	-119.686	-61.280	7.800	71.499
2	70.423	4.859	118.204	-70.423	-4.859	-69.496
3	41.280	-3.662	120.430	-41.280	3.662	-157.140
4	90.011	6.707	-121.913	-90.424	-.721	159.143
1	61.461	-6.215	-71.499	-61.574	7.410	57.812
2	70.274	6.676	69.496	-70.274	-6.676	-56.084
3	41.360	-2.595	157.140	-41.360	2.595	-162.354
4	90.275	3.056	-159.143	-90.488	-1.861	164.082
1	61.695	-6.329	-57.812	-62.064	9.608	13.708
2	70.146	7.907	56.084	-70.146	-7.907	-12.318
3	41.400	-1.869	162.354	-41.400	1.869	-172.701
4	90.442	3.448	-164.082	-90.811	-.169	174.091
1	62.202	-8.673	-13.708	-62.202	8.673	-8.151
2	70.020	8.562	12.318	-70.210	-7.475	8.396
3	41.423	-1.246	172.701	-41.423	1.246	-175.841
4	90.799	1.536	-174.091	-90.987	-.048	176.086
1	62.437	-6.780	8.151	-62.437	6.780	-76.801
2	67.751	9.608	-8.396	-70.893	-3.678	75.636
3	41.442	.013	175.841	-41.442	-.013	-175.714
4	90.946	2.811	-176.086	-91.888	3.115	174.549
1	62.677	-3.994	76.801	-62.677	3.994	-117.576

LIVE LOAD ANALYSIS (4 LOAD CASES)

WHITNEY'S ARCH

Case Results

oad ase	Axial @ LJ (kips)	Shear @ LJ (kips)	BM @ LJ (K-ft)	Axial @ GJ (kips)	Shear @ GJ (kips)	BM @ GJ (K-ft)
2	70.659	6.829	-75.636	-71.864	-.951	115.347
3	41.400	1.857	175.714	-41.400	-1.857	-156.760
4	91.935	.978	-174.549	-93.140	4.900	154.531
1	62.771	-2.021	117.576	-62.771	2.021	-127.965
2	71.798	3.211	-115.347	-72.493	-.292	124.350
3	41.321	3.158	156.760	-41.321	-3.158	-140.530
4	93.248	-1.968	-154.531	-93.943	4.887	136.914
1	62.801	-.603	127.965	-62.801	.603	-131.082
2	72.466	1.930	-124.350	-73.226	.972	126.824
3	41.239	4.090	140.530	-41.239	-4.090	-119.388
4	94.029	-2.764	-136.914	-94.790	5.666	115.129
1	62.790	1.320	131.082	-62.790	-1.320	-117.320
2	73.224	1.270	-126.824	-74.921	4.485	110.066
3	41.095	5.351	119.388	-41.095	-5.351	-63.597
4	94.919	-2.761	-115.129	-96.616	8.516	56.344
1	62.680	3.941	117.320	-62.680	-3.941	-75.682
2	75.043	-1.352	-110.066	-76.980	[illegible]	65.781
3	40.835	7.063	63.597	-40.835	-7.063	11.022
4	96.888	-4.474	-56.344	-98.824	10.153	-20.923
1	62.469	6.472	75.682	-62.469	-6.472	-6.291
2	77.201	-3.913	-65.781	-79.366	9.509	-6.174
3	40.517	8.708	-11.022	-40.517	-8.708	104.386
4	99.154	-6.149	20.923	-101.318	11.745	-116.851
1	62.174	8.869	6.291	-62.174	-8.869	90.309
2	79.672	-6.451	6.174	-82.051	11.939	-106.434
3	40.152	10.259	-104.386	-40.152	-10.259	216.128
4	101.695	-7.841	116.851	-104.073	13.349	-232.252
1	61.793	11.222	-90.309	-61.793	11.222	214.662
2	82.445	-8.837	106.434	-85.031	14.252	-234.363
3	39.734	11.775	-216.128	-39.734	-11.775	346.615
4	104.505	-9.391	232.252	-107.070	14.805	-366.316

Printer Banner Goes Here

LIVE LOAD ANALYSIS (4 LOAD CASES)

WHITNEY'S ARCH

*** JOINT DISPLACEMENTS ***

Case Results

Joint Number	Load Case	X-Displ. (in)	Y-Displ. (in)	Rotation (rad)
1	1	0.00000	0.00000	0.00000
	2	0.00000	0.00000	0.00000
	3	0.00000	0.00000	0.00000
	4	0.00000	0.00000	0.00000
2	1	-.01912	.03715	.00055
	2	.01788	-.04136	-.00060
	3	.04714	-.10133	-.00154
	4	-.04839	.09713	.00149
3	1	-.05454	.11607	.00071
	2	.05406	-.12925	-.00079
	3	.14903	-.33977	-.00231
	4	-.14952	.32681	.00223
4	1	-.08602	.19400	.00055
	2	.08730	-.21952	-.00066
	3	.26052	-.63097	-.00243
	4	-.25925	.60545	.00233
5	1	-.10238	.23811	.00016
	2	.10570	-.2781[illegible]	-.00028
	3	.35227	-.9029[illegible]	-.00202
	4	-.34875	.86285	.00190
6	1	-.10025	.22648	-.00036
	2	.10531	-.28202	.00024
	3	.40919	-1.09901	-.00120
	4	-.40414	1.04347	.00107
7	1	-.09293	.19608	-.00065
	2	.09666	-.25952	.00052
	3	.42347	-1.15521	-.00067
	4	-.41774	1.09176	.00054
8	1	-.08234	.14889	.00092
	2	.08055	-.22052	.00078
	3	.42363	-1.1767[illegible]	-.00011
	4	-.42232	1.10706	-.00002
9	1	-.05503	.00745	-.00137
	2	.06181	-.0[illegible]	.00125
	3	.41[illegible]	-1.[illegible]	.00[illegible]
	4	-.40885	1.03[illegible]	-.001[illegible]
10	1	-.02756	-.17125	-.00158
	2	.03376	.07075	.00149
	3	.38295	-.91505	.00221
	4	-.37676	.81859	-.00230

< Printer Banner Goes Here >

LIVE LOAD ANALYSIS (4 LOAD CASES)

WHITNEY'S ARCH

Case Results

Joint Number	Load Case	X-Displ. (in)	Y-Displ. (in)	Rotation (rad)
11	1	-.02180	-.21874	-.00156
	2	.02769	.11537	.00148
	3	.37379	-.84907	.00245
	4	-.36789	.74570	-.00255
12	1	-.01107	-.32004	-.00147
	2	.01617	.21063	.00138
	3	.35336	-.67179	.00289
	4	-.34825	.56238	-.00298
13	1	-.00804	-.35452	-.00140
	2	.01281	.24306	.00132
	3	.34646	-.60068	.00301
	4	-.34169	.48941	-.00310
14	1	.00013	-.49092	-.00083
	2	.00250	.37174	.00078
	3	.31900	-.21478	.00333
	4	-.31637	.09560	-.00336
15	1	0.00000	-.54154	0.00000
	2	0.00000	.41960	0.00000
	3	.30949	.17959	.00316
	4	-.30949	-.30152	-.00316
16	1	-.00013	-.49092	.00083
	2	-.00250	.37174	-.00078
	3	.31631	.52819	.00259
	4	-.31894	-.64737	-.00255
17	1	.00804	-.35452	.00140
	2	-.01281	.24306	-.00132
	3	.33378	.79346	.00180
	4	-.33855	-.90492	-.00171
18	1	.01107	-.32004	.00147
	2	-.01617	.21063	-.00138
	3	.33756	.83458	.00163
	4	-.34262	-.94397	-.00154
19	1	.02180	-.21874	.00158
	2	.02767	.11537	-.00148
	3	.34738	.92611	.00114
	4	-.35327	-1.02943	-.00105
20	1	.02756	-.17125	.00158
	2	-.02876	.07079	-.0014[illegible]
	3	.35110	.95686	.00091
	4	-.35730	-1.05732	-.00081
21	1	.05503	.00945	.00137

LIVE LOAD ANALYSIS (4 LOAD CASES)

WHITNEY'S ARCH

Case Results

Joint Number	Load Case	X-Displ. (in)	Y-Displ. (in)	Rotation (rad)
	2	-.06181	-.09668	-.00125
	3	.35931	1.01375	.00004
	4	-.36609	-1.10099	.00008
22	1	.08234	.14889	.00092
	2	-.08865	-.22052	-.00078
	3	.34971	.97105	-.00074
	4	-.35602	-1.04269	.00087
23	1	.09293	.19608	.00065
	2	-.09866	-.25953	-.00052
	3	.33640	.91690	-.00106
	4	-.34214	-.98035	.00119
24	1	.10025	.22648	.00036
	2	-.10531	-.28202	-.00024
	3	.31694	.84424	-.00135
	4	-.32200	-.89977	.00148
25	1	.10238	.23811	-.00016
	2	-.10573	-.27816	.00028
	3	.26077	.65669	-.00174
	4	-.26408	-.69674	.00186
26	1	.08602	.19400	-.00055
	2	-.08730	-.21952	.00066
	3	.18569	.45906	-.00184
	4	-.18697	-.46458	.00195
27	1	.05454	.11607	-.00071
	2	-.05406	-.12925	.00079
	3	.10316	.22791	-.00162
	4	-.10267	-.24109	.00170
28	1	.01912	.03715	-.00055
	2	-.01788	-.04136	.00060
	3	.03222	.06561	-.00102
	4	-.03098	-.06982	.00107
29		0.00000	0.00000	0.00000
	2	0.00000	0.00000	0.00000
	3	0.00000	0.00000	0.00000
	4	0.00000	0.00000	0.00000

LIVE LOAD ANALYSIS (4 LOAD CASES)

WHITNEY'S ARCH

*** SUPPORT REACTIONS ***

Case Results

Joint Number	Load Case	X-Reaction (kips)	Y-Reaction (kips)	Z-Reaction (K-ft)
1	1	60.598	16.500	-214.662
	2	70.591	49.500	234.363
	3	40.930	46.305	547.655
	4	90.259	19.695	-527.955
29	1	-60.598	16.500	214.662
	2	-70.591	49.500	-234.363
	3	-40.930	6.495	346.615
	4	-90.259	59.505	-366.316

CRITICAL LOAD ON WHITNEY ARCH

***** MEMBER LOAD DATA *****

ase 1 - member distributed loads

em .	Sloped UDL K/ft slope	Proj. UDL K/ft horiz	Local UDL k/ft perp	Local UDL K/ft parll	Triangular K/ft @ GJ	Thermal Change (F)
1	0	-23.5	0	0	0	0
2	0	-23.5	0	0	0	0
3	0	-23.5	0	0	0	0
4	0	-23.5	0	0	0	0
5	0	-23.5	0	0	0	0
6	0	-23.5	0	0	0	0
7	0	-23.5	0	0	0	0
8	0	-23.5	0	0	0	0
9	0	-23.5	0	0	0	0
0	0	-23.5	0	0	0	0
1	0	-23.5	0	0	0	0
2	0	-23.5	0	0	0	0
3	0	-23.5	0	0	0	0
4	0	-23.5	0	0	0	0
5	0	-23.5	0	0	0	0
6	0	-23.5	0	0	0	0
7	0	-23.5	0	0	0	0
8	0	-23.5	0	0	0	0
9	0	-23.5	0	0	0	0
0	0	-23.5	0	0	0	0
1	0	-23.5	0	0	0	0
2	0	-23.5	0	0	0	0
3	0	-23.5	0	0	0	0
4	0	-23.5	0	0	0	0
5	0	-23.5	0	0	0	0
6	0	-23.5	0	0	0	0
7	0	-23.5	0	0	0	0
8	0	-23.5	0	0	0	0

oped UDL, Projected UDL & Point Loads act in the global coordinate system.
cal Perpendicular, Local Parallel, Triangular Loads act in
e local member coordinate system.
iangular Loads are 0 at the lower joint with the magnitude specified at
e greater joint.

CRITICAL LOAD ON PARABOLIC ARCH

WHITNEY'S ARCH

*** JOINT DISPLACEMENTS ***

Case Results

Joint Number	Load Case	X-Displ. (in)	Y-Displ. (in)	Rotation (rad)
1	1	0.00000	0.00000	0.00000
2	1	-.04866	-.16462	-.00183
3	1	-.01909	-.51629	-.00320
4	1	.05002	-.99971	-.00413
5	1	.12996	-1.56879	-.00470
6	1	.19793	-2.17521	-.00482
7	1	.22448	-2.48533	-.00506
8	1	.24696	-2.80579	-.00520
9	1	.26556	-3.41666	-.00460
10	1	.24262	-3.93464	-.00372
11	1	.23091	-4.04874	-.00366
12	1	.20001	-4.28527	-.00331
13	1	.18682	-4.36562	-.00322
14	1	.10299	-4.66788	-.00171
15	1	0.00000	-4.77585	0.00000
16	1	-.10299	-4.66788	.00171
17	1	-.18682	-4.36562	.00322
18	1	-.20001	-4.28527	.00331
19	1	-.23091	-4.04874	.00366
20	1	-.24262	-3.93464	.00372
21	1	-.26556	-3.41666	.00460
22	1	-.24696	-2.80579	.00520
23	1	-.22448	-2.48533	.00506
24	1	-.19793	-2.17521	.00482
25	1	-.12996	-1.56879	.00470

CRITICAL LOAD ON PARABOLIC ARCH

WHITNEY'S ARCH

Case Results

Joint Number	Load Case	X-Displ. (in)	Y-Displ. (in)	Rotation (rad)
26	1	-.05002	-.99971	.00413
27	1	.01909	-.51629	.00320
28	1	.04866	-.16462	.00183
29	1	0.00000	0.00000	0.00000

CRITICAL LOAD ON WHITNEY ARCH

*** JOINT DISPLACEMENTS ***

Case Results

Joint Number	Load Case	X-Displ. (in)	Y-Displ. (in)	Rotation (rad)
1	1	0.00000	0.00000	0.00000
2	1	-.33012	.40387	.00688
3	1	-.89038	1.37969	.00962
4	1	-1.45051	2.48996	.00913
5	1	-1.87802	3.39780	.00628
6	1	-2.12684	3.87432	.00194
7	1	-2.18403	3.89519	-.00086
8	1	-2.19963	3.74565	-.00373
9	1	-2.14320	2.96761	-.00885
10	1	-2.03244	1.59980	-.01357
11	1	-2.00495	1.16961	-.01479
12	1	-1.95114	.10760	-.01710
13	1	-1.93647	-.31791	-.01787
14	1	-1.91131	-2.61165	-.01989
15	1	-1.99977	-5.01194	-.01969
16	1	-2.18664	-7.23630	-.01708
17	1	-2.43349	-9.00986	-.01235
18	1	-2.48345	-9.29158	-.01129
19	1	-2.61526	-9.92319	-.00805
20	1	-2.66847	-10.13806	-.00654
21	1	-2.82642	-10.50458	.00018
22	1	-2.83337	-10.06358	.00679
23	1	-2.76211	-9.56067	.00969
24	1	-2.63772	-8.88741	.01237
25	1	-2.21944	-7.08717	.01691

Case Results

Joint Number	Load Case	X-Displ. (in)	Y-Displ. (in)	Rotation (rad)
26	1	-1.59238	-4.85981	.01892
27	1	-.86867	-2.61023	.01736
28	1	-.23086	-.77844	.01128
29	1	0.00000	0.00000	0.00000

*** JOINT DATA ***

r	X - coord. (feet)	Y - coord. (feet)	X - Degree of Freedom	Y - Degree of Freedom	Z - Degree of Freedom
	0	0	0	0	0
	9.919	4.963	1	1	1
	19.87	9.438	1	1	1
	29.84	13.43	1	1	1
	39.83	16.92	1	1	1
	49.84	19.92	1	1	1
	54.86	21.24	1	1	1
	59.88	22.42	1	1	1
	69.92	24.43	1	1	1
	79.94	25.95	1	1	1
	82.45	26.25	1	1	1
	87.96	26.8	1	1	1
	89.98	26.96	1	1	1
	100	27.48	1	1	1
	110	27.5	1	1	1
	120	27.08	1	1	1
	129.98	26.22	1	1	1
	131.98	26	1	1	1
	137.46	25.31	1	1	1
	139.95	24.97	1	1	1
	149.94	23.31	1	1	1
	159.92	21.22	1	1	1
	164.88	20.02	1	1	1
	169.86	18.72	1	1	1
	179.83	15.82	1	1	1
	189.89	12.49	1	1	1
	199.87	8.774	1	1	1
	209.99	4.583	1	1	1
	220	0	0	0	0

Degree of Freedom: 0=restrained 1=free j=coupled to joint 'j'

Thesis
K264 Kelley
c.1 Safety and stability in
concrete barrel shell roof
structures.